Pharmacology, Biochemistry and Behavior 179 (2019) 156–170

Contents lists available at ScienceDirect

Pharmacology, Biochemistry and Behavior

journal homepage: www.elsevier.com/locate/pharmbiochembeh

Amantadine enhances nigrostriatal and mesolimbic dopamine function in the rat brain in relation to motor and exploratory activity

Susanne Nikolaus[a,*], Hans-Jörg Wittsack[b], Markus Beu[a], Christina Antke[a], Hubertus Hautzel[c], Frithjof Wickrath[d], Anja Müller-Lutz[b], Maria Angelica De Souza Silva[e], Joseph P. Huston[e], Gerald Antoch[b], Hans-Wilhelm Müller[a]

[a] Clinic of Nuclear Medicine, University Hospital Düsseldorf, Heinrich Heine University, Moorenstr. 5, D-40225 Düsseldorf, Germany
[b] Department of Diagnostic and Interventional Radiology, University Hospital Düsseldorf, Heinrich Heine University, Moorenstr. 5, D-40225 Düsseldorf, Germany
[c] Clinic for Nuclear Medicine, University Hospital Essen, Hufelandstraße 55, D-45122 Essen, Germany
[d] Institute for Clinical Diabetology, German Diabetes Center (DDZ), Heinrich-Heine University, Auf'm Hennekamp 65, 40225 Düsseldorf, Germany
[e] Center for Behavioural Neuroscience, Institute of Experimental Psychology, Heinrich-Heine University, Universitätsstr. 1, D-40225 Düsseldorf, Germany

ARTICLE INFO

Keywords:
$D_{2/3}$ receptor
[^{123}I]IBZM
Amantadine
NMDA receptor
Small animal SPECT

ABSTRACT

Purpose: The present study assessed the influence of the NMDA receptor (R) antagonist amantadine (AMA) on cerebral dopamine $D_{2/3}$R binding in relation to motor and exploratory activity in the rat.
Methods: $D_{2/3}$R binding was determined in anaesthetized animals with small animal SPECT in baseline and after challenge with AMA (10 or 40 mg/kg) using [^{123}I]IBZM as radioligand. Immediately post-challenge and prior to radioligand administration, motor/exploratory behaviors were assessed for 30 min in an open field. Each rat underwent measurements with a dedicated small animal MRI in order to gain anatomical information. Regions of interest were defined on SPECT-MRI overlays. The regional binding potentials in baseline and post-challenge were estimated by computing ratios of the specifically bound compartments to the cerebellar reference region.
Results: 40 mg/kg AMA reduced $D_{2/3}$R binding in nucleus accumbens, caudateputamen and thalamus, while 10 mg/kg decreased $D_{2/3}$R binding in the anterodorsal hippocampus. The higher dose decreased ambulatory activity, rearing and grooming, but elevated sitting and head-shoulder motility relative to both vehicle and the lower dose in the first 15 min post-challenge.
Conclusions: Results showed reductions of $D_{2/3}$R binding in regions of the nigrostriatal and mesolimbic system after challenge with AMA, which reflect an increased availability of dopamine. Thereby, an inverse relationship between nigrostriatal and mesolimbic dopamine and motor/exploratory activity can be inferred. Findings may be relevant for the treatment of neurological and psychiatric conditions such as Parkinson's disease, Huntington's disease or schizophrenia, which are characterized by both dopaminergic and glutamatergic dysfunction.

1. Introduction

Alterations of glutamate (GLU) function have been linked to numerous neurological and psychiatric conditions including Parkinson's, Huntington's, and Alzheimer's disease, major depressive disorder, schizophrenia, attention-deficit hyperactivity disorder and epilepsy (for review see Kornhuber and Weller, 1997; Konradi and Heckers, 2003; Mitchell and Baker, 2010; Archer and Garcia, 2016; Vishnoi et al., 2016; Rebec, 2018). GLU is the main excitatory neurotransmitter in the central nervous system. Together with the inhibitory γ-amino butyric acid (GABA), it serves to modulate nigrostriatal and mesolimbic dopamine (DA) function.

Amantadine (AMA; 1-amino-adamantane), a synthetic tricyclic amine, is a low-affinity uncompetitive NMDA receptor (R) antagonist, which binds to the phencyclidine-binding site (inhibition constant [K_i] = 10 μM; Kornhuber et al., 1991). With an affinity in the same order of magnitude, AMA also binds to the opiate σ_1R (K_i = 20 μM Kornhuber et al., 1993).

AMA is mainly applied for the treatment of L-DOPA induced dyskinesia and psychiatric symptoms of Parkinson's disease (for review see Vanle et al., 2018). However, it has also proved beneficial in multiple sclerosis fatigue (Shaygannejad et al., 2012), major depressive disorder (Moryl et al., 1993), traumatic brain injury (Spritzer et al., 2015) and refractory electrial status epilepticus (Wilson et al., 2018).

* Corresponding author.
E-mail address: susanne.nikolaus@uni-duesseldorf.de (S. Nikolaus).

https://doi.org/10.1016/j.pbb.2018.12.010
Received 24 October 2018; Received in revised form 11 December 2018; Accepted 27 December 2018
Available online 11 January 2019
0091-3057/

In rats, AMA (40 and 80 mg/kg intraperitonelly [i.p.], Maj et al., 1972; 50 and 100 mg/kg subcutaneously [s.c.], Buus Lassen, 1973; 100 mg/kg i.p., Bak et al., 1972) increased motor activity starting "a few minutes after administration" with a maximum effect after 60 min (Maj et al., 1972). Thereby, elevated motor behavior after 50 and 100 mg/kg AMA included locomotion, rearing, sniffing, head twitches and spells of rapid grooming (Buus Lassen, 1973). A lower dose (20 mg/kg i.p.) had no effect, whereas a higher one (160 mg/kg i.p.) even depressed motor behavior (Maj et al., 1972). However, Buus Lassen (1973) reported that a dose of 25 mg/kg s.c. did not affect motility within the first 4 h after administration, but decreased it at 4 to 6 h post-injection.

As of yet, the central action of AMA is a matter of debate. In rats, the application of 100 mg/kg i.p. elevated striatal acetylcholine (ACh) and nigral and striatal GABA (Bak et al., 1972), starting immediately post-injection. Elevation of striatal DA and serotonin (5-HT) levels were detectable, but not significant in the study of Bak et al. (1972). Likewise, Maj et al. (1972) did not observe changes in striatal DA after 10 to 80 mg/kg AMA i.p. Contrarily, Takahashi et al. (1996) described a significant increase of striatal DA after 100 mg/kg AMA i.p. immediately post-injection. Moreover, intrastriatal infusion of AMA (0.1 mM and 1 mM) elicited both DA and GLU efflux in the striatum (Takahashi et al., 1996). An augmentation of striatal DA was also observed by Scatton et al. (1970) after s.c. application of 40 mg/kg AMA, and by Quack et al. (1995) after i.p. application of 46 or 92 mg/kg AMA.

Two in vivo imaging studies of striatal D_2R-like binding have been performed on Parkinsonian patients after chronic treatment with AMA (200 mg/day for at least 10 days) using [^{11}C]raclopride as radioligand (Volonté et al., 2001; Moresco et al., 2002). In both studies, striatal D_2R-like binding significantly increased, indicating that, at least in Parkinsonian patients, the AMA-induced elevation of synaptic DA was not high enough to induce a detectable competition with the exogenous radioligand. However, so far, no in vivo imaging study has been performed on D_2R-like binding in healthy humans or rats after acute treatment with AMA.

We have previously shown that the $GABA_A$R agonist muscimol reduced motor/exploratory behaviors (Nikolaus et al., 2017) as well as radioligand binding to the D_2R-like subtype in caudateputamen (CP), nucleus accumbens (NAC), thalamus (THAL), substantia nigra/ventral tegmental area (SN/VTA) and posterior hippocampus (pHIPP) in the rat relative to baseline (Nikolaus et al., 2018a, 2018b). We employed a two-modality in vivo imaging approach, in which images of D_2R-like binding were coregistered with morphological images obtained with a dedicated small animal MRI. This allowed transference of the pre-defined cortical and subcortical volumes of interest (VOIs) of the Paxinos standard rat brain MRI (Schiffer et al., 2006) to the functional SPECT images and, thus, permitted analysis of radioligand binding to D_2R-like binding sites in numerous brain regions beyond the CP (Nikolaus et al., 2018a, 2018b).

In the present study, we assessed the effect of AMA challenge (10 and 40 mg/kg i.p.) on motor/exploratory behaviors and on D_2R-like binding in regions of the rat nigrostriatal and mesolimbic systems, which are related to motor behavior and both cognitive and emotional functioning (NAC, CP, THAL, SN/VTA, frontal cortex [FC], motor cortex [MC], parietal cortex [PC], anteriodorsal hippocampus [aHIPP], pHIPP) using small animal SPECT and MRI.

2. Materials and methods

2.1. Animals

Imaging studies of D_2R-like binding sites were conducted on 47 adult male Wistar rats (ZETT, Heinrich-Heine University, Düsseldorf, Germany), weighing 400 ± 43 g (mean ± standard deviation [SD]; age: 3–4 months). The animals underwent behavioral testing after injection of AMA (10 mg/kg: n = 22; 40 mg/kg: n = 25), morphological imaging (n = 41) and SPECT measurements in baseline (n = 38) and after injection of AMA (10 mg/kg: n = 19; 40 mg/kg: n = 18). A total of 7 rats merely underwent behavioral measurements without D_2R imaging, since they exhibited seizures (n = 2) or suffered a cardial arrest (n = 5) during or shortly after the administration of the anaesthetic. Behavioral data obtained after AMA were compared to the behavioral data obtained after vehicle (0.9% saline) in 16 further male rats of the same strain, age (3–4 months) and weight (418 ± 63 g) at the same time of the year (September until November). Behavioral data obtained after saline were previously published (Nikolaus et al., 2016, 2017).

Rats were maintained in standard macrolon cages (590 × 380 × 200 mm; 3 animals per cage) in a climate cabinet (Scantainer, Scanbur BK, Karslunde, Denmark; temperature: 20–22 °C; air humidity: 60–70%) with an artificial light-dark cycle (lights on at 6:00 a.m., lights off at 6:00 p.m.) and food and water freely available. Temperature and air humidity were checked on a daily basis. The study was carried out in accordance with the recommendations of the "Principles of laboratory animal care" (NIH publication No. 86-23, revised 1985) and the German Law on the Protection of Animals. The protocol was approved by the regional authority (Landesamt für Natur, Umwelt und Verbraucherschutz, Nordrhein-Westfalen, Recklinghausen, Germany).

2.2. MRI studies

Upon anaesthesia with ketaminehydrochloride (Ketavet®, Pharmacia GmbH, Erlangen, BRD; dose: 50 mg/kg i.p., concentration: 100 mg/ml) and xylazinehydrochloride (Rompun®, Bayer, Leverkusen, BRD; dose: 2.5 mg/kg i.p., concentration: 20 mg/ml), rat heads were scanned with a dedicated small animal MRI (MRS3000 Pre-clinical MRI, 3.0 T, MR Solutions, Guildford, UK; cylindric volume coil with an inner diameter of 54 mm; field of view: 64 × 64 × 44 mm; spatial resolution: 0.25 × 0.25 × 0.69 mm) as previously described (Nikolaus et al., 2018a). High-resolution anatomical images in coronal slice orientation were obtained by performing a 3D fast low angle shot (FLASH) sequence (repetition time: 30 ms; echo time: 4.87 ms; excitation flip angle: 30°; total acquisition time: 553 s; Haase et al., 1986). The initial 192 × 192 × 96 image matrix was interpolated by zero-filling to a 256 × 256 × 128 matrix before reconstruction.

2.3. Drug treatment

A total of 47 rats received i.p. injection of AMA hydrochloride (Sigma-Aldrich, Taufkirchen, Germany; molecular weight: 151.25 g/mol; n = 22: dose, 10 mg/kg, concentration; 10 mg/ml; n = 25: dose, 40 mg/kg, concentration; 40 mg/ml). Sixteen additional rats were pretreated with vehicle (0.9% saline; B. Braun Melsungen AG, Melsungen, Germany; dose: 1 ml/kg; Nikolaus et al., 2016, 2017).

The dose of 40 mg/kg AMA had formerly been shown to be behaviorally active in rats after systemic application (Maj et al., 1972). The dosage of 10 mg/kg was chosen, since it lies in the range of doses applied to Parkinsonian patients (200 to 1000 mg/day [~3 to 14 mg/kg]; Kornhuber et al., 1995). In rats, an increase of motor activity had been observed immediately post-challenge (Maj et al., 1972). This also holds for the rise of striatal DA after i.p. or intracranial administration (Quack et al., 1995; Takahashi et al., 1996). Therefore, behavioral measurements were started immediately after application of AMA.

2.4. SPECT studies

Imaging of D_2R-like binding sites in baseline and after i.p. injection of 10 and 40 mg/kg AMA was performed as previously described (e.g., Nikolaus et al., 2016, 2017). After completion of behavioral tests, animals were anaesthetized with ketaminehydrochloride (dose: 100 mg/

kg i.p., concentration: 100 mg/ml) and xylazinehydrochloride (dose: 5 mg/kg i.p., concentration: 20 mg/ml).

The employed radioligand [^{123}I]S-3-iodo-N-(1-ethyl-2-pyrrolidinyl) methyl-2-hydroxy-6-methoxy benzamide ([^{123}I]IBZM) has a high affinity for binding sites of the D_2R-like subtype (D_2: K_i = 1.6 nM, D_3: K_i = 2.2 nM; Videbaek et al., 2000). Besides, studies on the benzamide analogue [^{11}C]raclopride have shown similar affinities for the high- and low-affinity state of the D_2R-like subtype (Seneca et al., 2006). From this may be inferred that also [^{123}I]IBZM binds to D_2R-like binding sites in both configurations and that the regional binding potentials (BPs) obtained in the present investigation reflect the regional densities of $D_{2/3}$Rs as such, irrespective of the individual contributions of either affinity state.

[^{123}I]IBZM (GE Healthcare, München, Germany; activity: 25.4 ± 3.6 MBq, concentration: 3.4×10^{-9} g/ml, specific activity: > 74 TBq/mmol at reference time) was injected into the lateral tail vein. Previous studies on humans and rats had shown that specific binding of [^{123}I]IBZM in the striatum reaches a plateau at about 40 min post-injection, which remains stable for up to 2 h (Verhoeff et al., 1991). This coincides with the time of maximum striatal DA concentrations after i.p. application of AMA (60 to 90 min post-challenge, Takahashi et al., 1996). Hence, SPECT measurements were started 45 min after radioligand administration (75 min post-challenge).

The employed small animal tomograph ("TierSPECT"; field of view: 90 mm; sensitivity: 22 and 16 cps/MBq for ^{99m}T and ^{123}I, respectively; spatial resolution: 2.8 and 3.44 mm for ^{99m}TC and ^{123}I, respectively) was described in detail elsewhere (Schramm et al., 2000). Data were acquired over 60 min; thus, animals were kept under anaesthesia for a total of 105 min.

MRI scans and SPECT measurements in baseline and after challenge were performed in randomized order and were separated by at least 3 days to allow for recovery.

2.5. Behavioral studies

Immediately after i.p. application of AMA (10 or 40 mg/kg) or vehicle (0.9% saline; B. Braun Melsungen AG, Melsungen, Germany; dose: 1 ml/kg), rats underwent behavioral measurements in an open field (Phenotyper®, Noldus Information Technology, Wageningen, The Netherlands; dimensions: 45 × 45 × 56 cm) as previously described (e.g., Nikolaus et al., 2016, 2017). The animals had not been previously habituated to the open field. Durations (s) and frequencies (n) of the following motor and exploratory behaviors were rated in blocks of 5 min for a total of 30 min using EthoVision XT (Noldus Information Technology, Wageningen, The Netherlands): (A) ambulation as a measure of motor activity; (B) sitting as a measure of "passive immobility" (Müller et al., 2004); (C) rearing (freely standing or leaning against the wall) as a measure of both motor and exploratory activity; (D) head-shoulder motility, while the animal remained in a sitting position, as a measure of exploratory activity (Nikolaus et al., 2013); (E) grooming (fur, paw and claw licking, scratching). Behavioral studies were performed between 9:00 a.m. and 5:00 p.m.

2.6. Evaluation of SPECT imaging studies

$D_{2/3}$R imaging data were evaluated with PMOD (version 3.5, PMOD Technologies Ltd., Zürich, Switzerland) as previously described (Nikolaus et al., 2018a). Firstly, for each rat, SPECT and MR images were coregistered. The MR image of each rat was then coregistered with the Paxinos standard rat brain MRI (Schiffer et al., 2006) provided by PMOD, and the necessary mathematical transformations were saved. Using these transformations, the SPECT image as coregistered with the MRI was re-imported, which allowed creation of an overlay with the Paxinos standard rat brain MRI. On these overlays, the following VOIs were defined: CP, NAC, THAL, SN/VTA, FC, MC, PC, aHIPP and pHIPP. All these regions have maximum craniocaudal (CC) and one-sided mediolateral (ML) and dorsoventral (DV; vertical or oblique) dimensions in the range of or beyond the spatial resolution of the small animal SPECT: CP, CC: > 4.5 mm, ML: ~ 3.4 mm, DV: ~ 5 mm; NAC, CC: > 3 mm, ML: ~ 2.5 mm, DV: ~ 3 mm; THAL, CC: > 6.0 mm, ML: ~ 4.5 mm, DV: ~ 3.5 mm; SN/VTA, CC: > 2.5 mm, ML: ~ 2.8 mm, DV: ~ 3.2 mm; FC, CC: > 3.4 mm, ML: ~ 3.1 mm, DV: ~ 3.8 mm; MC, CC: > 8.4 mm, ML: ~ 4.0 mm, DV: ~4.2 mm; PC, CC: > 7.8 mm, ML: ~3.0 mm, DV: ~ 8.0 mm; HIPP, CC: > 8 mm, ML: ~ 5.0 mm, DV: ~ 6.5 mm (Paxinos and Watson, 2014).

Since [^{123}I]IBZM accumulation in the cerebellum (CER) is non-specific, the CER was used as reference region. Estimations of regional BPs were obtained according to the simplified reference tissue model by computing ratios of radioactivity counts obtained in the specifically-bound compartments (CP, NAC, THAL, SN/VTA, FC, MC, PC, aHIPP and pHIPP) to radioactivity counts in the CER (Ichise et al., 2001).

2.7. Statistical analysis

2.7.1. $D_{2/3}$R imaging studies

Distributions of both regional BPs and behavioral data were tested for normality with the non-parametric Kolmogorov-Smirnov test ($\alpha \leq 0.05$). Neither in baseline, nor after either dose of AMA, were regional BPs uniformly normally distributed ($.002 \leq p \leq .200$).

Medians and interquartile ranges (25-/75- and 5-/95-percentiles) were computed for regional BPs. Regional BPs were compared between baseline and challenge (10 or 40 mg/kg mg/kg AMA) with the Wilcoxon signed rank test for paired samples (two-tailed, $\alpha \leq 0.05$) and between AMA doses with the Mann-Whitney *U* test for independent samples (two-tailed, $\alpha \leq 0.05$). Moreover, percentual differences of BPs after AMA in either dose relative to baseline and of BPs after 10 relative to 40 mg/kg AMA were computed. Calculations were performed with IBM SPSS Statistics 23 (IBM SPSS Software Germany, Ehningen, Germany).

2.7.2. Behavioral studies

Distributions of behavioral data (duration [s] and frequency [n] of ambulation, sitting, rearing, head-shoulder motility and grooming) in 5-min bins were assessed with the non-parametric Kolmogorov-Smirnov test ($\alpha \leq 0.05$). Since in the pre-treatment conditions (10 and 40 mg/kg AMA, saline) numerous behavioral parameters were not normally distributed ($.0001 \leq p \leq .200$), behaviors in each 5-min time bin and over the whole trial (min 1–30) were compared between groups with the Kruskal-Wallis test (two-sided, $\alpha \leq 0.05$) and with the Mann-Whitney *U* test (two-sided, $\alpha \leq 0.0167$ after Bonferroni correction for multiple comparisons). Calculations were performed with IBM SPSS Statistics 23 (IBM SPSS Software Germany, Ehningen, Germany).

Since our rationale was to gain information on the temporal dynamics of behavioral alterations, the medians of the individual parameters obtained after saline (Y-axis: duration and frequency of ambulation, sitting, rearing, head-shoulder motility or grooming) were plotted against the end-points of the individual time frames (X-axis) as previously described (Nikolaus et al., 2016, 2017). Upon visual inspection of the time-behavior (t-b) curves, appropriate mathematical models were fit to the individual behavioral parameters, using either linear or non-linear regression analysis, with the regression coefficient (R^2) as a measure for the goodness of fit. The same models were fit to the behavioral data obtained after 10 and 40 mg/kg AMA (Table 1). Curves were fit using GraphPad Prism (version 3.0 for Windows, GraphPad Software, San Diego, USA). T-b curves were compared between treatment groups (10 and 40 mg/kg AMA vs saline) using the *F* test ($\alpha \leq 0.0167$ after Bonferroni correction for multiple comparisons).

Table 1
Best-fit values and regression coefficients (R^2) of time-behavior curves after treatment with saline, 10 mg/kg amantadine and 40 mg/kg amantadine.

Behavioral parameter	Model	Saline		10 mg/kg amantadine		40 mg/kg amantadine	
Ambulation duration	Exponential function:	a	196.3	a	112.5	a	157.0
	$y(t) = a * \exp(-K * t) + plateau$	K	0.128	K	0.058	K	0.225
	with t, time; a, initial value at t = 0; K, rate constant	Plateau	11.48	Plateau	−1.381	Plateau	36.27
		R^2	0.982	R^2	0.974	R^2	0.865
Ambulation frequency	Exponential function:	a	63.96	a	56.51	a	81.18
	$y(t) = a * \exp(-K * t) + plateau$	K	0.102	K	0.040	K	0.274
	with t, time; a, initial value at t = 0; K, rate constant	Plateau	2.609	Plateau	−7.105	Plateau	13.71
		R^2	0.964	R^2	0.937	R^2	0.853
Sitting duration	Quadratic function:	a	−36.16	a	140.7	a	93.50
	$y(t) = a + bt + ct^2$	b	7.961	b	−14.49	b	−2.246
	with t, time, a, absolute term; b, linear term; c, quadratic term	c	−0.039	c	0.488	c	−0.024
		R^2	0.922	R^2	0.969	R^2	0.930
Sitting frequency	Quadratic function:	a	−2.276	a	11.60	a	7.30
	$y(t) = a + bt + ct^2$	b	1.359	b	−0.713	b	0.879
	with t, time, a, absolute term; b, linear term; c, quadratic term	c	−0.036	c	−0.024	c	−0.032
		R^2	0.965	R^2	0.942	R^2	0.849
Rearing duration	Cubic function:	a	35.67	a	−24.67	a	42.0
	$y(t) = a + bt + ct^2 + dt^3$	b	3.847	b	14.97	b	−6.778
	with t, time; a, absolute term; b, linear term; c, quadratic term; d,	c	−0.469	c	−0.957	c	0.354
	cubic term	d	0.011	d	0.017	d	−0.006
		R^2	0.992	R^2	0.997	R^2	0.981
Rearing frequency	Exponential function:	a	40.59	a	38.87	a	208.1
	$y(t) = a * \exp(-K * t) + plateau$	K	0.140	K	0.054	K	0.640
	with t, time; a, initial value at t = 0; K, rate constant	Plateau	1.899	Plateau	−5.927	Plateau	1.528
		R^2	0.977	R^2	0.938	R^2	0.921
Duration of head-shoulder	Quadratic function:	a	112.5	a	88.70	a	90.45
motility	$y(t) = a + bt + ct^2$	b	0.020	b	2.164	b	4.250
	with t, time, a, absolute term; b, linear term; c, quadratic term	c	−0.048	c	−0.096	c	−0.028
		R^2	0.966	R^2	0.847	R^2	0.988
Frequency of head-shoulder	Linear function:	a	−1.120	a	−0.926	a	−0.623
motility	$y(t) = at + b$	b	46.93	b	48.20	b	43.42
	with t, time; a, slope and b, y-intercept	R^2	0.931	R^2	0.919	R^2	0.816
Grooming duration	Quadratic function:	a	5.455	a	−49.57	a	−4.876
	$y(t) = a + bt + ct^2$	b	1.810	b	10.08	b	1.168
	with t, time, a, absolute term; b, linear term; c, quadratic term	c	−0.037	c	−0.245	c	−0.014
		R^2	0.758	R^2	0.897	R^2	0.962
Grooming frequency	Exponential function:	a	0.200	a	−2.278	a	−3.80
	$y(t) = a + bt + ct^2$	b	0.196	b	0.546	b	0.871
	with t, time, a, absolute term; b, linear term; c, quadratic term	c	−0.004	c	−0.014	c	−0.026
		R^2	0.671	R^2	0.980	R^2	0.942

3. Results

3.1. $D_{2/3}R$ binding

Fig. 1(A) and (B) show images of the Paxinos standard rat brain MRI atlas (Schiffer et al., 2006) at different positions from Bregma together with the standard VOI templates provided by PMOD (left columns). Middle and right columns display characteristic images of regional [^{123}I]IBZM accumulation on coronal slices in baseline (middle columns) and after challenge with 10 and 40 mg/kg AMA (right columns in Fig. 1A and B, respectively) in the same rats at the positions from Bregma depicted in the left columns (Paxinos and Watson, 2014).

After 10 mg/kg AMA (Fig. 2), the BP was significantly reduced in the aHIPP relative to baseline (−16%, p = .05). There were no differences between 10 mg/kg AMA and baseline in NAC, CP, THAL, SN/VTA, FC, MC, PC and pHIPP (.085 ≤ p ≤ .711).

After 40 mg/kg AMA (Fig. 3), the BP was significantly diminished in NAC (−5%, p = .008), CP (−7%, p = .049) and THAL (−12%, p = .020) compared to baseline. There were no differences between 40 mg/kg AMA and baseline in SN/VTA, FC, MC, PC, aHIPP and pHIPP (.109 ≤ p ≤ .438).

3.2. Motor and exploratory behaviors

The Kruskal-Wallis test yielded significant between-group differences for the following variables: ambulation duration in min 1–5, 10–15 and 25–30 (0.002 ≤ p ≤ 0.04), ambulation frequency in min 1–5, 10–15 and 25–30 (0.001 ≤ p ≤ 0.037), sitting duration in min 1–5, 6–10,11–15, 21–25 and 26–30 (0.0001 ≤ p ≤ 0.046), sitting frequency in min 1–5, 6–10, 11–15 and 1–30 (0.0001 ≤ p ≤ 0.018), rearing duration in min 1–5, 6–10, 11–15 and 1–30 (p ≤ 0.0001, each), rearing frequency in min 1–5, 6–10, 11–15 and 1–30 (0.0001 ≤ p ≤ 0.001), duration of head-shoulder motility in min 1–5, 6–10, 16–20, 21–25, 26–30 and 1–30 (0.0001 ≤ p ≤ 0.047), frequency of head-shoulder motility in min 11–15 and 26–30 (0.002 ≤ p ≤ 0.010), grooming duration in min 1–5 and 16–20, (0.0001 ≤ p ≤ 0.026), grooming frequency in min 1–5 (p ≤ 0.0001).

3.2.1. Ambulation

After 10 mg/kg AMA, ambulation was performed for a shorter time relative to saline in the first time bin (p < 0.0001; Fig. 4A). Ambulation duration after 40 mg/kg was lower compared to 10 mg/kg in min 11–15 (p = 0.012), but was increased relative to the lower dose in min 26–30 (p = 0.013). T-b curves did not differ between treatments (0.033 ≤ p ≤ 0.124; see Table 1 and inset Fig. 4A).

Ambulation frequency (Fig. 4B) after 40 mg/kg was reduced relative to the lower dose in min 6–10 (p = 0.001) and 11–15 (p < 0.0001). T-b curves did not differ between groups (0.094 ≤ p ≤ 0.147; see Table 1 and inset Fig. 4B).

3.2.2. Sitting

Sitting duration (Fig. 5A) after 10 mg/kg AMA was higher relative to saline in the first time bin (p < 0.0001). After 40 mg/kg rats exhibited more sitting in min 1–5 (p = 0.002), but less sitting during the

A

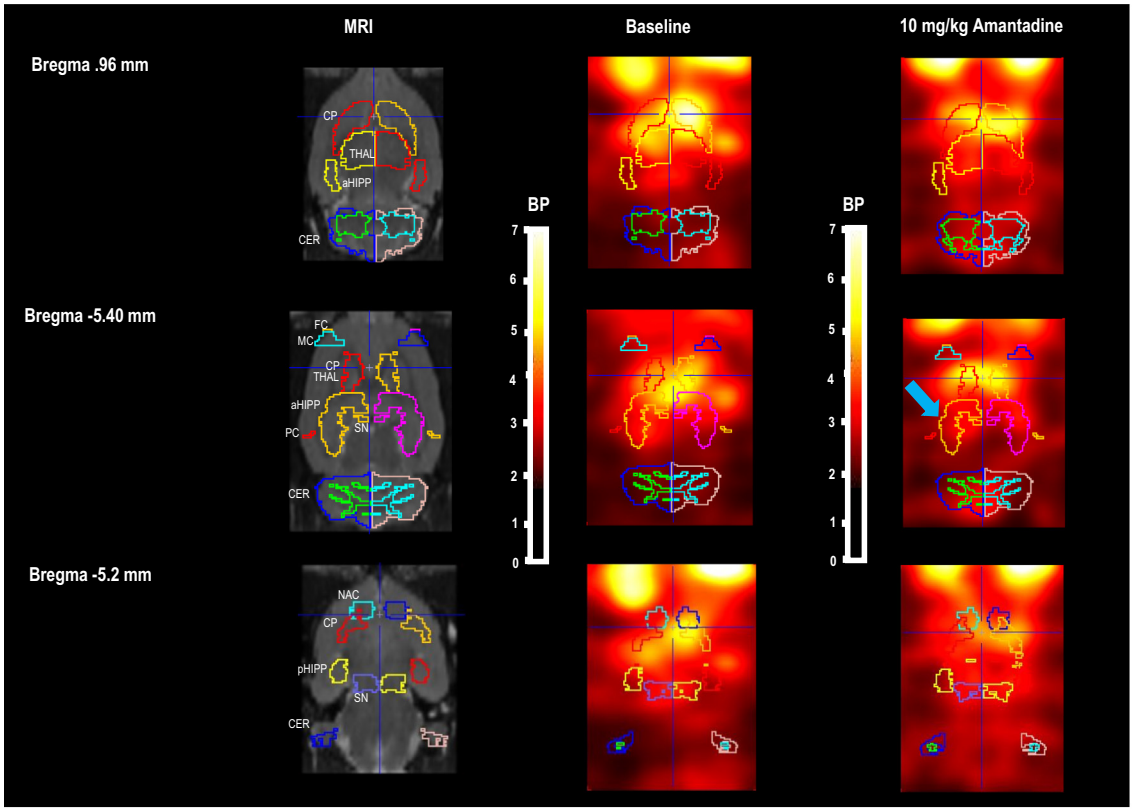

B

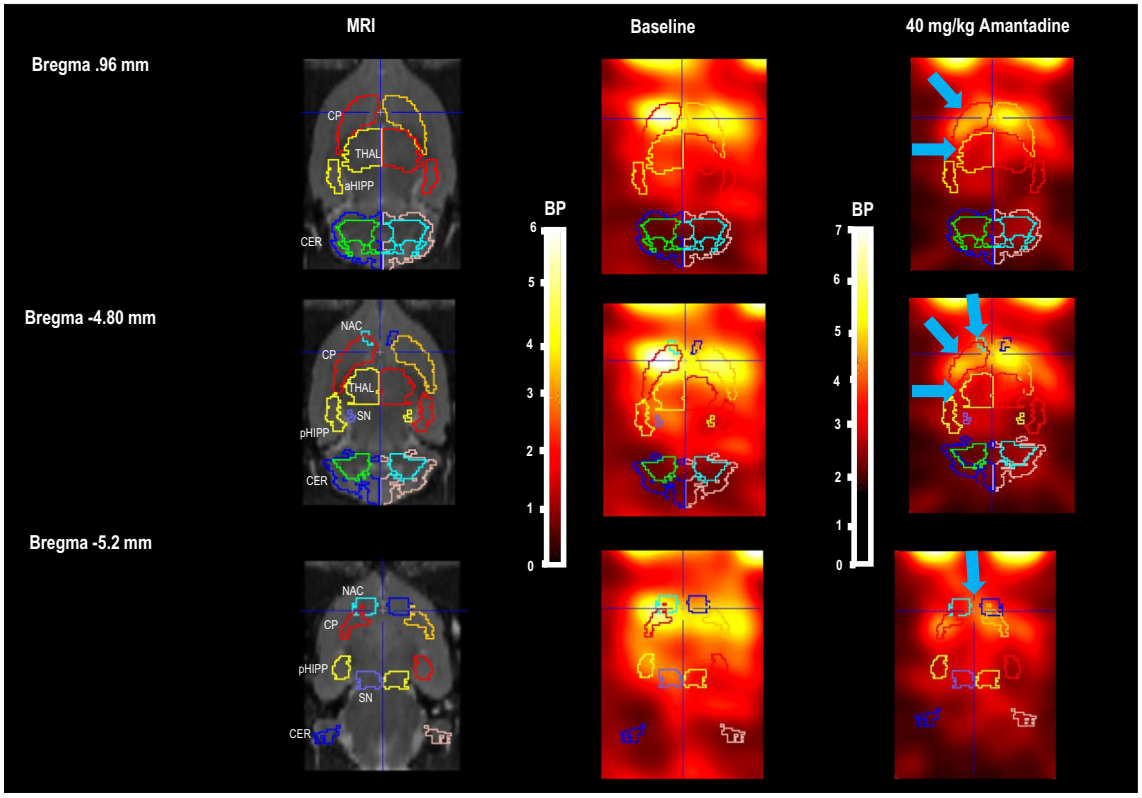

(caption on next page)

Fig. 1. Paxinos standard rat brain MRI and individual $D_{2/3}R$ SPECT in baseline and after challenge with (A) 10 mg/kg amantadine, and (B) 40 mg/kg amantadine with [^{123}I]IBZM as radioligand. *Left columns*: Paxinos standard rat brain MR images (Schiffer et al., 2006) at different positions from Bregma together with the standard VOI templates provided by PMOD. *Middle columns*: Series of coronal SPECT slices in a characteristic rat in baseline at the same positions from Bregma. *Right columns:* SPECT slices in the same rat after 10 mg/kg AMA at the same positions from Bregma. The reduction of [^{123}I]IBZM accumulation in the anterodorsal hippocampus is marked by a blue arrow. All SPECT images show binding potentials (BP). It is understood, that the calculation of BPs is only valid for regions with specific radioligand binding. Image algebra was performed with PMOD (version 3.5, PMOD Technologies Ltd., Zürich, Switzerland).
Abbreviations (in alphabetical order): aHIPP, anterodorsal hippocampus, CER, cerebellum; CP, caudateputamen; FC, frontal cortex; MC, motor cortex; NAC, nucleus accumbens; PC, parietal cortex; pHIPP, posterior hippocampus; SN/VTA, substantia nigra/ventral tegmental area; THAL, thalamus. (For interpretation of the references to color in this figure legend, the reader is referred to the web version of this article.)

last 5 min ($p = 0.007$) compared to saline. After the higher dose, sitting duration was higher in min 11–15 ($p = 0.004$) and 21–25 ($p = 0.001$), but lower in the last time bin ($p < 0.0001$) relative to the lower dose. T-b curves (Table 1) differed between 40 mg/kg AMA and saline ($p = 0.009$) as well as between AMA doses ($p = 0.001$): while sitting duration was initially low and rose constantly after saline, it was higher after both AMA doses (see inset Fig. 5A). Thereby, after 10 mg/kg, it declined over the first and increased again over the second half of the testing time, while, after 40 mg/kg, it declined from the beginning.

Sitting frequency (Fig. 5B) after 10 mg/kg AMA was higher relative to saline in the first ($p < 0.001$) and in the last time bin ($p = 0.001$). Moreover, after 40 mg/kg, rats exhibited sitting behavior more frequently in min 1–5 and 6–10 ($p < 0.0001$, both). After 40 mg/kg, sitting frequency was higher compared to the lower dose in min 6–10 ($p < 0.0001$) and 11–15 ($p = 0.008$). However, it was lower compared to 10 mg/kg in the last time bin ($p = 0.002$). T-b curves (Table 1) differed between 10 mg/kg AMA and saline ($p = 0.006$) as well as between AMA doses ($p = 0.003$). After saline, sitting frequency during the first time bin was lower relative to both AMA doses (see inset Fig. 5B). Moreover, it reached a lower vertex later compared to 40 mg/kg AMA. Furthermore, after the higher dose, sitting frequency rose over the first half and declined over the second half of the testing time, whereas after the lower dose, it decreased over the first and an increased again over the second half of the testing session.

3.2.3. Rearing

After 40 mg/kg AMA, rats reared for a shorter time (Fig. 6A) compared to both saline and 10 mg/kg AMA in min 1–5 ($p < 0.0002$ and $p = 0.013$, respectively), 6–10 ($p < 0.0001$, both) and 11–15 ($p < 0.0001$, both) as well as when pooled over the whole 30 min ($p = 0.001$ and $p < 0.0001$, respectively). T-b curves (Table 1) differed between treatment groups: after saline, rearing duration during the first time bin was highest, decreased over the following 20 min and slightly increased again during the last 5 min of the testing session (see inset Fig. 6A). After 40 mg/kg AMA, rearing duration during the first 5 min was lowest, 6decreased further over the following 10 min and increased again over the last 15 min of the testing session. After 10 mg/kg, rearing duration was higher compared to 40 mg/kg, increased over

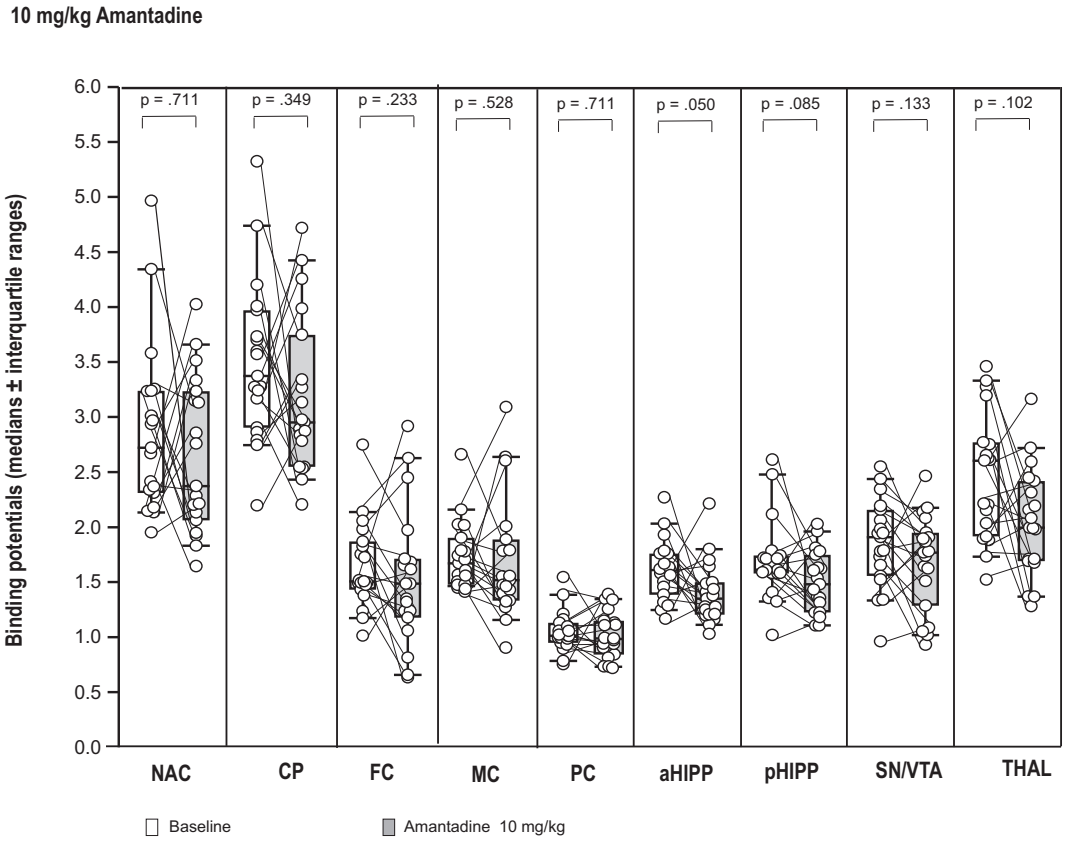

Fig. 2. Binding potentials in baseline (white) and after challenge with 10 mg/kg amantadine (grey). Rendered are medians and 25-/75- (boxes) and 9-/95-quartiles (whiskers). The circles represent the individual animals. For the paired comparisons, the respective p values are given (Wilcoxon signed rank test for paired samples, two-tailed, $\alpha = 0.05$).
Abbreviations (in alphabetical order): aHIPP, anterodorsal hippocampus; CP, caudateputamen; FC, frontal cortex; MC, motor cortex; NAC, nucleus accumbens; PC, parietal cortex; pHIPP, posterior hippocampus; prefrontal cortex; SN/VTA, substantia nigra/ventral tegmental area; THAL, thalamus.

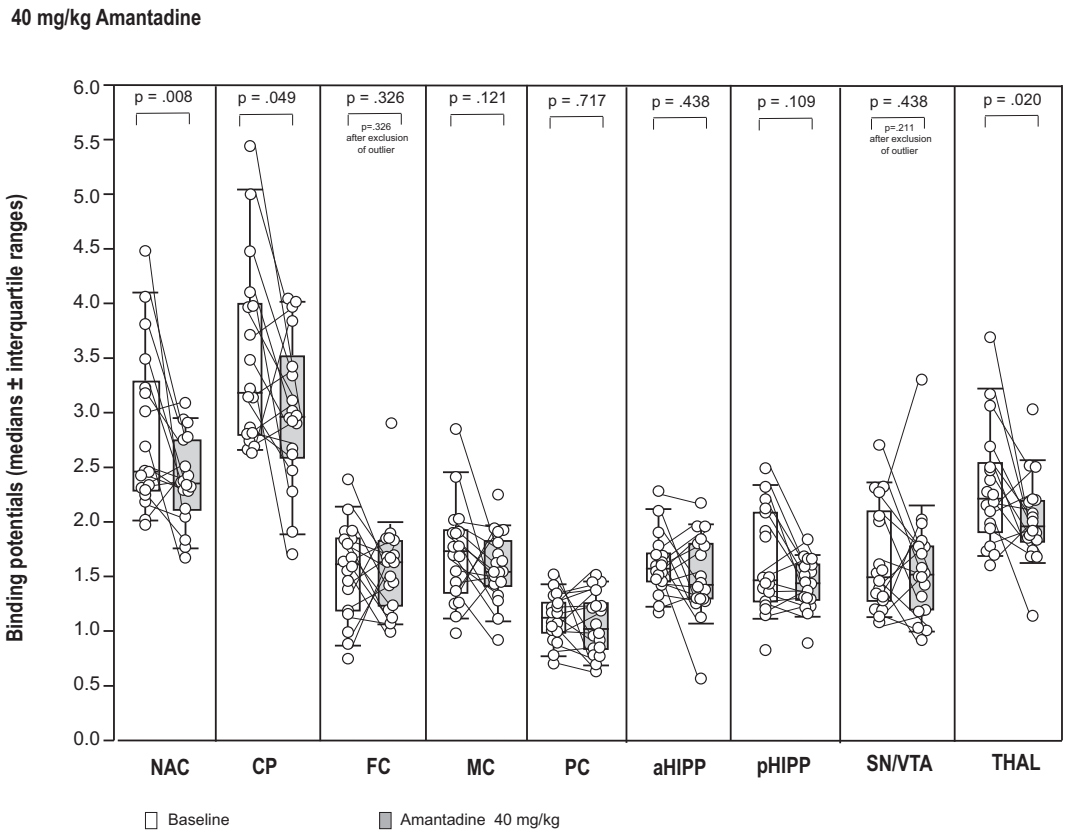

Fig. 3. Binding potentials in baseline (white) and after challenge with 40 mg/kg amantadine (grey). Rendered are medians and 25-/75- (boxes) and 9-/95-quartiles (whiskers). The circles represent the individual animals. For the paired comparisons, the respective p values are given (Wilcoxon signed rank test for paired samples, two-tailed, $\alpha = 0.05$).
Abbreviations (in alphabetical order): aHIPP, anterodorsal hippocampus; CP, caudateputamen; FC, frontal cortex; MC, motor cortex; NAC, nucleus accumbens; PC, parietal cortex; pHIPP, posterior hippocampus; prefrontal cortex; SN/VTA, substantia nigra/ventral tegmental area; THAL, thalamus.

the following 5 min and declined again over the following 20 min (10 mg/kg vs saline: $p = 0.003$; 40 mg/kg vs saline: $p = 0.0004$; 10 mg/kg vs 40 mg/kg: $p < 0.0001$).

After 40 mg/kg AMA, rats reared less frequently (Fig. 6B) compared to saline in min 1–5, 6–10 and 11–15 min as well as when pooled over the whole testing session ($p < 0.0001$, each; Fig. 6B). After the higher dose, rearing frequency was reduced relative to the lower dose in min 6–10 and 11–15 min as well as when pooled over the whole testing session ($p < 0.0001$, each). T-b curves (Table 1) differed between 40 mg/kg AMA and saline ($p = 0.001$) as well as between AMA doses ($p = 0.003$). After saline and 10 mg/kg AMA, rearing frequency over time was higher and declined at a lower rate relative to the higher AMA dose (see inset Fig. 6B).

3.2.4. Head-shoulder motility

After 40 mg/kg AMA, animals moved their heads and shoulders for a longer time compared to saline in min 16–20, 21–25 and 26–30, as well as when pooled over the whole 30 min ($p < 0.0001$, each; Fig. 7A). Furthermore, heads and shoulders were moved for a longer time after 40 mg/kg relative to the lower dose of AMA in min 1–5 ($p < 0.0001$), 6–10 ($p = 0.016$), 16–20 ($p < 0.0001$), 21–25 ($p < 0.0001$) and 26–30 ($p < 0.0001$) as well as from min 1–30 ($p < 0.0001$). T-b curves (Table 1) differed between 40 mg/kg AMA and saline ($p = 0.0001$) as well as between AMA doses ($p < 0.0001$). While the duration of head-shoulder motility decreased after saline, it almost linearly increased over testing time after 40 mg/kg AMA, while, after the lower dose, it slightly rose until the end of the second time bin and then decreased until the end of the session (see inset of Fig. 7A).

After 10 mg/kg, rats moved their heads and shoulders more often compared to saline in min 11–15 ($p = 0.008$; Fig. 7B). After the higher dose, the frequency of head-shoulder movements was increased in min 26–30 relative to saline ($p = 0.003$). T-b curves did not differ between treatment groups ($0.032 \leq p \leq 0.405$; see Table 1 and inset Fig. 7B).

3.2.5. Grooming

After both 10 and 40 mg/kg AMA, animals groomed for a shorter time in the first time bin relative to saline ($p < 0.0001$, each; Fig. 8A). Moreover, grooming was reduced after the higher compared to the lower dose in min 16–20 ($p = 0.009$) as well as when pooled over the whole 30 min ($p = 0.016$). T-b curves did not differ between treatment groups ($0.020 \leq p \leq 0.127$; see Table 1 and inset Fig. 8A).

After both 10 and 40 mg/kg AMA, animals groomed less frequently in the first time bin relative to saline ($p < 0.0001$, each; Fig. 8B). T-b curves did not differ between treatment groups ($0.075 \leq p \leq 0.165$; see Table 1 and inset Fig. 8B).

4. Discussion

4.1. $D_{2/3}R$ binding

Challenge with the NMDAR antagonist AMA in a dose of 10 mg/kg significantly reduced $D_{2/3}R$ binding in the aHIPP (−16%), while 40 mg/kg AMA reduced $D_{2/3}R$ binding in NAC (−5%), CP (−7%) and THAL (−12%).

We have previously shown that challenge with the DA precursor L-DOPA (Nikolaus et al., 2016), the DA reuptake inhibitor methylphenidate (Nikolaus et al., 2005), the D_2R antagonist haloperidol (Nikolaus et al., 2005) and the $GABA_AR$ agonist muscimol (Nikolaus et al., 2017,

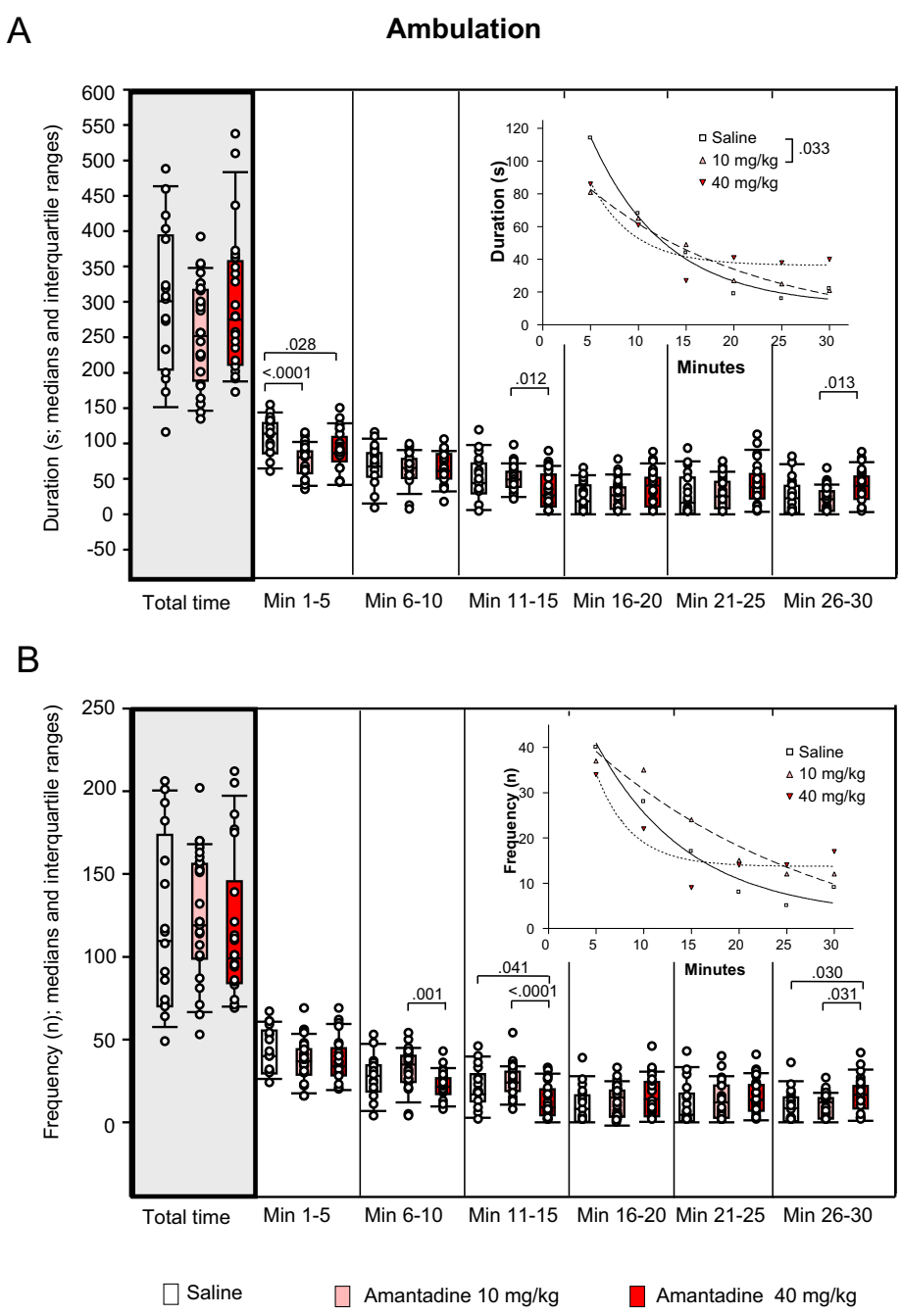

Fig. 4. Ambulation. Duration (s) and frequency (n) after vehicle (0.9% saline; white), 10 mg/kg amantadine (pink) and 40 mg/kg amantadine (red). The figure shows box and whisker plots of median ambulation durations (A) and frequencies (B) during the whole time of testing (grey shade) and in the individual 5-min time bins. 25-/75-percentiles are given in the boxes, while 5-/95-percentiles are represented by the whiskers. The circles represent the individual animals. Between-group differences were assessed using the Mann-Whitney *U* test (two-tailed). p values ≤ .05 are given in the figure. Due to the Bonferroni correction, p values ≤ .0167 are considered significant. *Inset*: Time-behavior curves (saline, white squares; 10 mg/kg amantadine pink triangles; 40 mg/kg amantadine, red triangles) obtained by plotting median values of ambulation durations (A) and ambulation frequencies (B) against time and fitting exponential functions [y (t) = a ∗ exp (−K ∗ x) + plateau with a, value at the time t; −K, rate constant; t, time] to these data. Between-group differences were assessed using the *F* test (two-tailed). p values ≤ .05 are given in the inset. Due to the Bonferroni correction, p values ≤ .0167 are considered significant. (For interpretation of the references to color in this figure legend, the reader is referred to the web version of this article.)

2018a, 2018b) decreased [^{123}]IBZM binding to the rat $D_{2/3}$R. Since all of these compounds enhance DA levels in the synaptic cleft and [^{123}]IBZM competes with endogenous DA molecules for $D_{2/3}$R binding sites (for review see Laruelle, 2000), the observed reductions of $D_{2/3}$R binding may be conceived to reflect elevations of synaptic DA. Hence, it can be inferred that, also in the present study, the decreases of $D_{2/3}$R binding in NAC, CP, THAL and aHIPP after AMA challenges were due to increased DA concentrations in these regions.

This is the first study, in which the effects of AMA on subcortical and neocortical DA were investigated using a non-invasive in vivo imaging method. Also, so far, the effect of AMA challenge on DA has only been studied in the CP. The present finding of elevated DA in the CP is consistent with the results of Scatton et al. (1970), Quack et al. (1995) and Takahashi et al. (1996) obtained after AMA doses between 40 and 100 mg/kg i.p. or s.c. However, they contradict the findings of Maj et al. (1972) as well as Bak et al. (1972), who did not find changes in striatal DA after 10 to 100 mg/kg AMA i.p. The precedent investigations either employed invasive in vivo methods such as microdialysis (Quack et al., 1995; Takahashi et al., 1996) or ex vivo methods such as spectrofluorometry of striatal tissue extracts (Bak et al., 1972; Maj et al., 1972) or ion exchange chromatography and liquid scintillation counting of striatal preparations (Scatton et al., 1970). In the study of Scatton et al. (1970), who found an increase of striatal DA, rats were killed 2 h after administration of AMA, whereas Bak et al. (1972) as well as Maj et al. (1972), who observed no significant effects, sacrificed their animals only 1 h post-challenge. It appears, thus, that a time of 1 h post-challenge is not sufficient to detect changes in DA levels, if combined with ex vivo methods, precluding AMA action in living compartments.

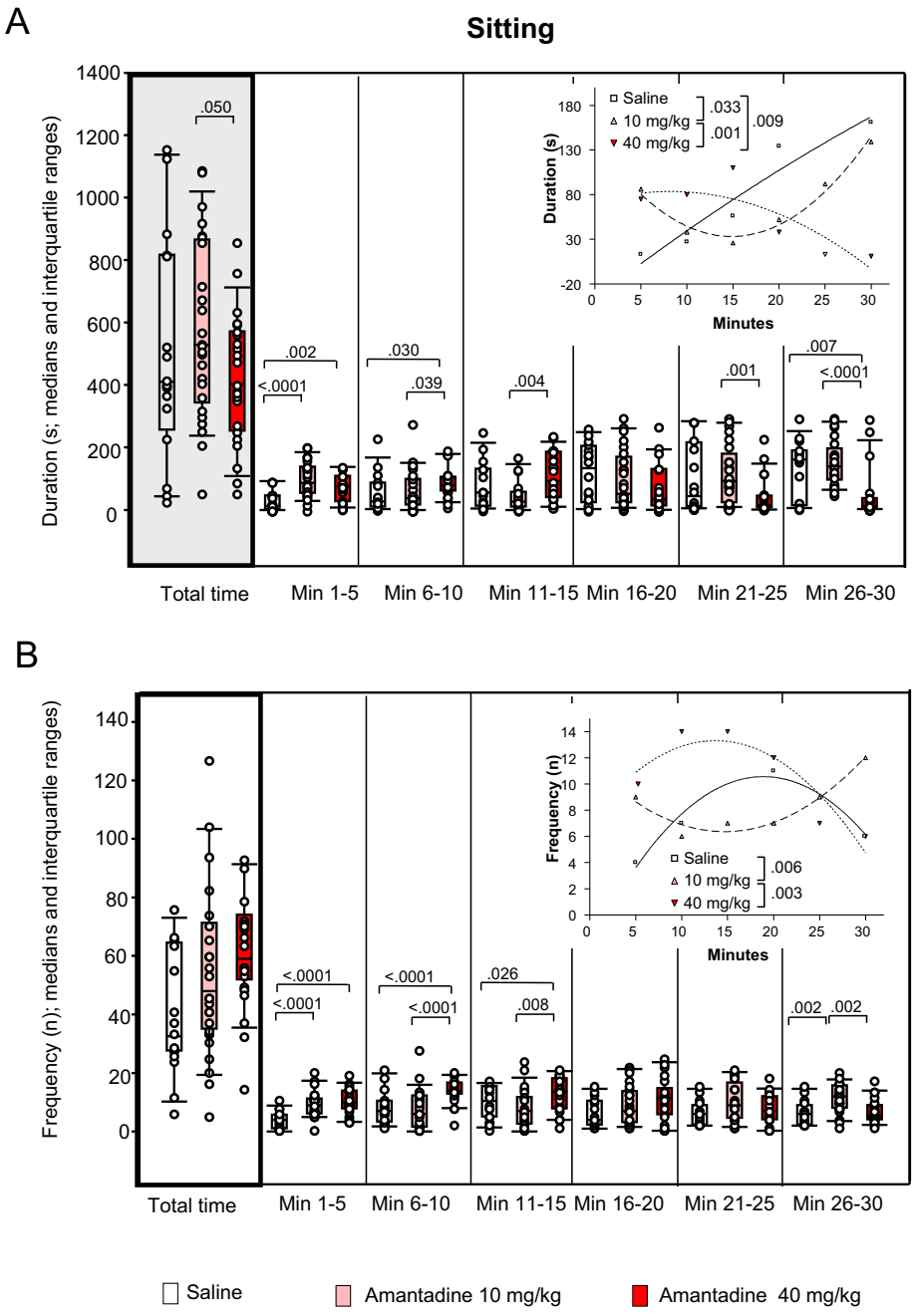

Fig. 5. Sitting. Duration (s) and frequency (n) after vehicle (0.9% saline; white), 10 mg/kg amantadine (pink) and 40 mg/kg amantadine (red). The figure shows box and whisker plots of median sitting durations (A) and frequencies (B) during the whole time of testing (grey shade) and in the individual 5-min time bins. 25-/75-percentiles are given in the boxes, while 5-/95-percentiles are represented by the whiskers. The circles represent the individual animals. Between-group differences were assessed using the Mann-Whitney *U* test (two-tailed). p values ≤ 0.05 are given in the figure. Due to the Bonferroni correction, p values ≤ 0.0167 are considered significant. *Inset*: Time-behavior curves (saline, white squares; 10 mg/kg amantadine, pink triangles; 40 mg/kg amantadine, red triangles) obtained by plotting median values of sitting durations (A) and sitting frequencies (B) against time and fitting quadratic functions [$y(t) = a + bt + ct^2$ with a, absolute term; b, linear term; c, quadratic term] to these data Between-group differences were assessed using the *F* test (two-tailed). p values ≤ 0.05 are given in the inset. Due to the Bonferroni correction, p values ≤ 0.0167 are considered significant. (For interpretation of the references to color in this figure legend, the reader is referred to the web version of this article.)

4.2. Motor and exploratory behaviors

In the dose of 10 mg/kg, AMA reduced motor and exploratory parameters (ambulation duration, rearing duration, duration of head-shoulder motility) as well as grooming relative to saline primarily in the first 5 min post-challenge. Consistently, parameters of passive immobility (sitting duration, sitting frequency) were elevated in the first bin.

After 40 mg/kg, motor parameters (ambulation duration and frequency) decreased during the first 15 min, but increased in min 25–30 (ambulation frequency) relative to saline. Parameters of passive immobility (sitting duration, sitting frequency) were elevated during the first 10 and 15 min, respectively. The parameters of more active exploration (rearing duration and frequency) decreased during the first 15 min, whereas the duration and frequency of mere head-shoulder movements, while the animals remained in a sitting position, increased during the last 15 min of testing time. As after the lower dose, the decline of grooming duration and frequency relative to saline was confined to the first 5 min.

The more intense and prolonged behavioral depression after the higher AMA dose is also illustrated by the t-b curves: after 40 mg/kg, the curves of ambulation duration and frequency had a lower level during the first 15 min post-challenge compared to the other treatments. Moreover, they declined at a faster rate relative to the curves obtained after treatment with 10 mg/kg AMA and saline. Similarly, after 40 mg/kg, the t-b curves of rearing frequency and rearing duration showed both lower initial values and lower levels as well as faster declines during the first 10 and 15 min, respectively, of the testing session.

The present results of decreased motor/exploratory activities after challenge with AMA are consistent with previous findings obtained after systemic treatment with the DA precursor L-DOPA (Nikolaus et al., 2016) or the $GABA_AR$ agonist muscimol (Nikolaus et al., 2017, 2018a,

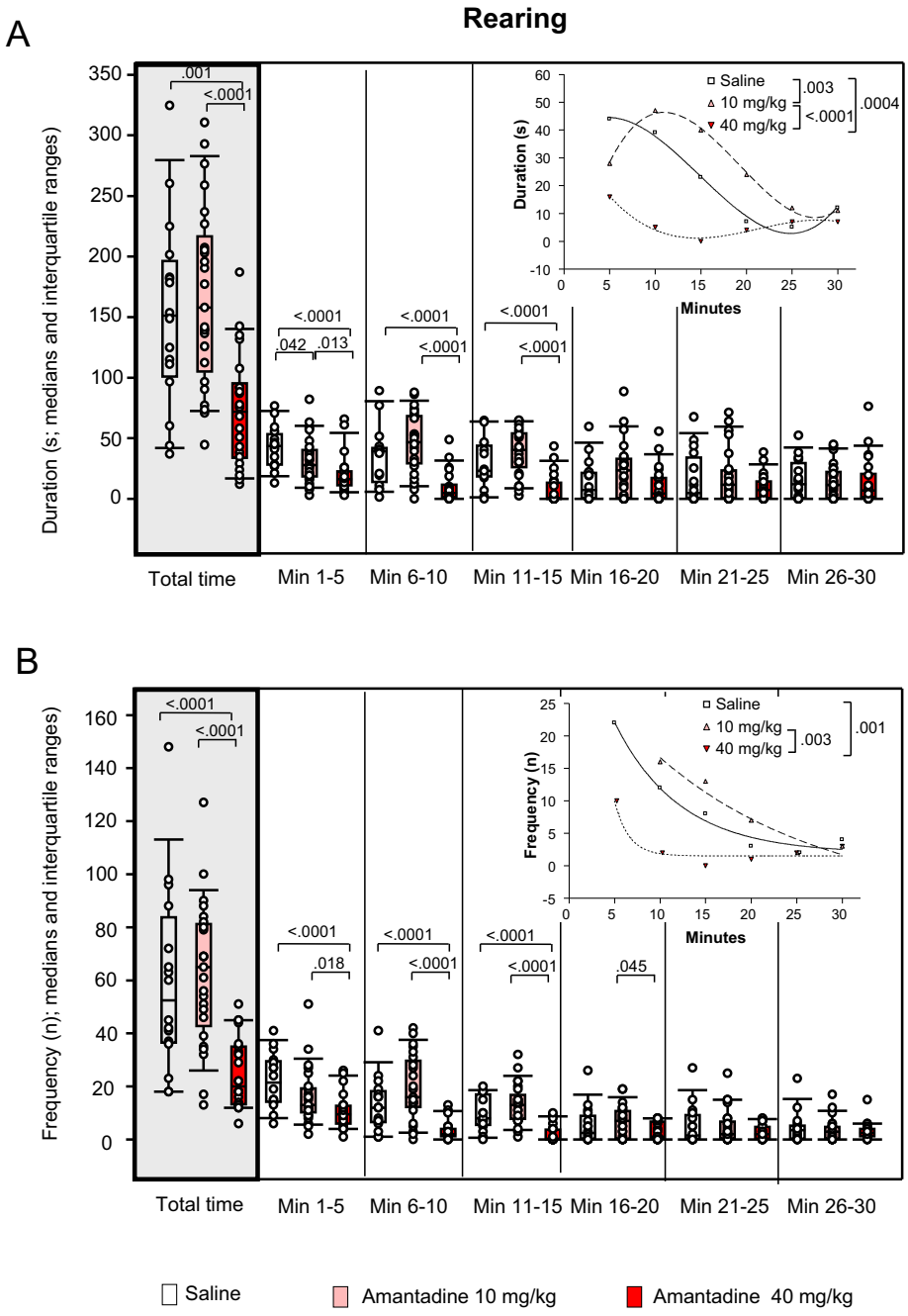

Fig. 6. Rearing. Duration (s) and Frequency (n) after vehicle (0.9% saline, white), 10 mg/kg amantadine (pink) and 40 mg/kg amantadine (red). The figure shows box and whisker plots of median rearing durations (A) and frequencies (B) during the whole time of testing (grey shade) and in the individual 5-min time bins. 25-/75-percentiles are given in the boxes, while 5-/95-percentiles are represented by the whiskers. The circles represent the individual animals. Between-group differences were assessed using the Mann-Whitney *U* test (two-tailed). p values ≤ 0.05 are given in the figure. Due to the Bonferroni correction, p values ≤ 0.0167 are considered significant. *Inset*: Time-behavior curves (saline, white squares; 10 mg/kg amantadine, pink triangles; 40 mg/kg amantadine, red triangles) obtained by plotting median values of rearing durations (A) and sitting frequencies (B) against time. Cubic function [$y(t) = a + bt + ct^2 + dt^3$ with a, absolute term; b, linear term; c, quadratic term; d, cubic term], were fit to the plots of rearing duration while exponential functions [$y(t) = a * \exp(-K * x)$ + plateau with a, value at the time t; −K, rate constant; t, time] were fit to the plots of rearing frequency. Between-group differences were assessed using the *F* test (two-tailed). p values ≤ 0.05 are given in the inset. Due to the Bonferroni correction, p values ≤ 0.0167 are considered significant. (For interpretation of the references to color in this figure legend, the reader is referred to the web version of this article.)

2018b), which are known to enhance DA levels in the synaptic cleft. However, they contradict precedent AMA studies on rats, which reported either no effect after systemic treatment with 20 mg/kg (Maj et al., 1972) or increased motor activity after administration of 40 to 100 mg/kg (Maj et al., 1972; Buus Lassen, 1973; Bak et al., 1972). Previous studies have revealed an age-dependency of motor function in the rat: L-DOPA, for instance, inhibited locomotor activity in adult animals (Fink and Smith, 1979; McDevitt and Setler, 1981), but accelerated motility in neonate, infant and adolescent rats (McDevitt and Setler, 1981; Grigoriadis et al., 1996; Navarrete et al., 2002). Thus, the most likely reason for the discrepancy between our findings and the results obtained by Maj et al. (1972), Buus Lassen (1973) and Bak et al. (1972) is the difference of ages between samples: in our study, animals were considerably older (approximately 4 months old and weighing 400 ± 43 g) compared to the other investigations, in which adolescent (110–115 g, Maj et al., 1972; 100–120 g, Buus Lassen, 1973: 100–120 g; average weight of 250 g, Bak et al., 1972) rats were employed. A further factor may have been the sex of the experimental animals (male rats in the present study, female rats by Buus Lassen, 1973, rats of either sex by Maj et al., 1972, no specification given by Bak et al. [1992]). Hormones such as testosterone and progesterone are behaviorally active and influence DA (de Souza Silva et al., 2008, 2009), NMDA and GABA function (Gibbs et al., 2006) in a variety of brain regions including NAC, CP and amygdala.

4.3. Mechanism of AMA action

The time course of behavioral effects suggests that, after either dose of AMA, DA concentrations started to rise immediately post-injection. However, only after the higher dose elevations of synaptic DA levels in NAC, CP and THAL were still visible at the time of SPECT measurements (min 75–135 post-challenge), whereas, after the lower dose,

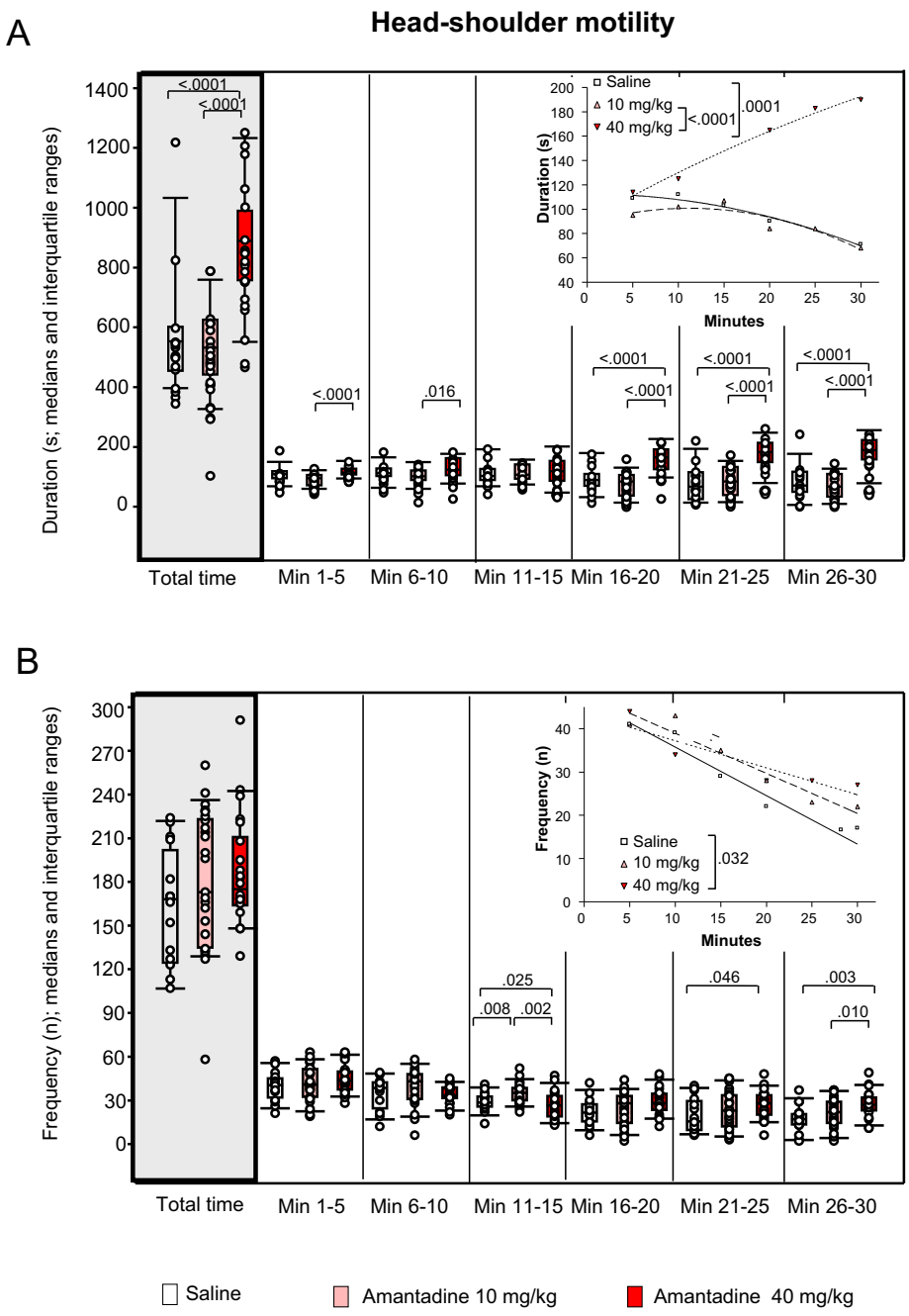

Fig. 7. Head-shoulder motility. Duration (s) and Frequency (n) after vehicle (0.9% saline, white), 10 mg/kg amantadine (pink) and 40 mg/kg amantadine (red). The figure shows box and whisker plots of the median durations (A) and frequencies (B) of head-shoulder motility during the whole time of testing (grey shade) and in the individual 5-min time bins. 25-/75-percentiles are given in the boxes, while 5-/95-percentiles are represented by the whiskers. The circles represent the individual animals. Between-group differences were assessed using the Mann-Whitney *U* test (two-tailed). p values ≤ 0.05 are given in the figure. Due to the Bonferroni correction, p values ≤ 0.0167 are considered significant. *Inset*: Time-behavior curves (saline, white squares; 10 mg/kg amantadine, pink triangles; 40 mg/kg amantadine, red triangles) were obtained by plotting median values of motility durations (A) and frequencies (B) against time. Quadratic functions [$y(t) = a + bx + cx^2$ with a, absolute term; bx, linear term; cx^2, quadratic term] were fit to the plots of motility durations, while linear functions [$y(t) = ax + b$ with a, slope and b, y-intercept] were fit to the plots of motility frequencies. Between-group differences were assessed using the *F* test (two-tailed). p values ≤ 0.05 are given in the inset. Due to the Bonferroni correction, p values ≤ 0.0167 are considered significant. (For interpretation of the references to color in this figure legend, the reader is referred to the web version of this article.)

effects on $D_{2/3}R$ binding could no longer be detected in these regions. The less intense and curtailed behavioral effects exerted by 10 mg/kg imply that regional DA releases were lower, leaving no impact on $D_{2/3}R$ binding after > 1 h post-injection. Notably, however, after the lower dose, a reduction of hippocampal $D_{2/3}R$ binding was found, which was not visible after 40 mg/kg AMA. This poses the question, exactly which effects on GLU, DA and GABA were triggered by either dose of AMA.

Since AMA elicits GLU release (Takahashi et al., 1996), and both CP and NAC receive GLUergic afferents (e.g. Johnson et al., 1968; Powell and Leman, 1976), for one, it may be hypothesized that the increased GLUergic input to the target regions of corticostriatal and corticomesolimbic projections augmented DA efflux in CP and NAC. On the other hand, AMA facilitates the release of GABA in CP and SN (Bak et al., 1972). Thus, it is as likely that the increased availability of inhibitory GABA in the neostriatal microcircuits (Groves, 1983) caused a reduction of DA efflux in the CP. In the DAergic system, DA concentrations are regulated by presynaptic autoreceptors of the D_2R-like subtype, which modulate DA synthesis and release via inhibitory feedback loops (Langer, 1974). Consequently, the decrease of neostriatal DA efflux likely reduced feedback inhibition, leading to an enhancement of DA release. Probably, GLUergic and GABAergic mechanisms of AMA action occur simultaneously, ultimately resulting in the net increase of synaptic DA reflected by the decline of neostriatal $D_{2/3}R$ binding relative to control after 40 mg/kg AMA.

The NAC sends GABAergic efferents to the VTA and to the ventral globus pallidus (GP). From the latter, further GABAergic projections extend to the THAL (Ueki et al., 1977; Yamamoto et al., 1983). Thus, it can be surmised that AMA also fascilitated the release of GABA in the NAC, leading to an inhibition of the GP and subsequent disinhibition of the THAL. The NAC receives inhibitory DAergic efferents from the latter region (Hara et al., 1989). The disinhibition of the THAL, thus, likely augmented the inhibitory DAergic input to the NAC, entailing a

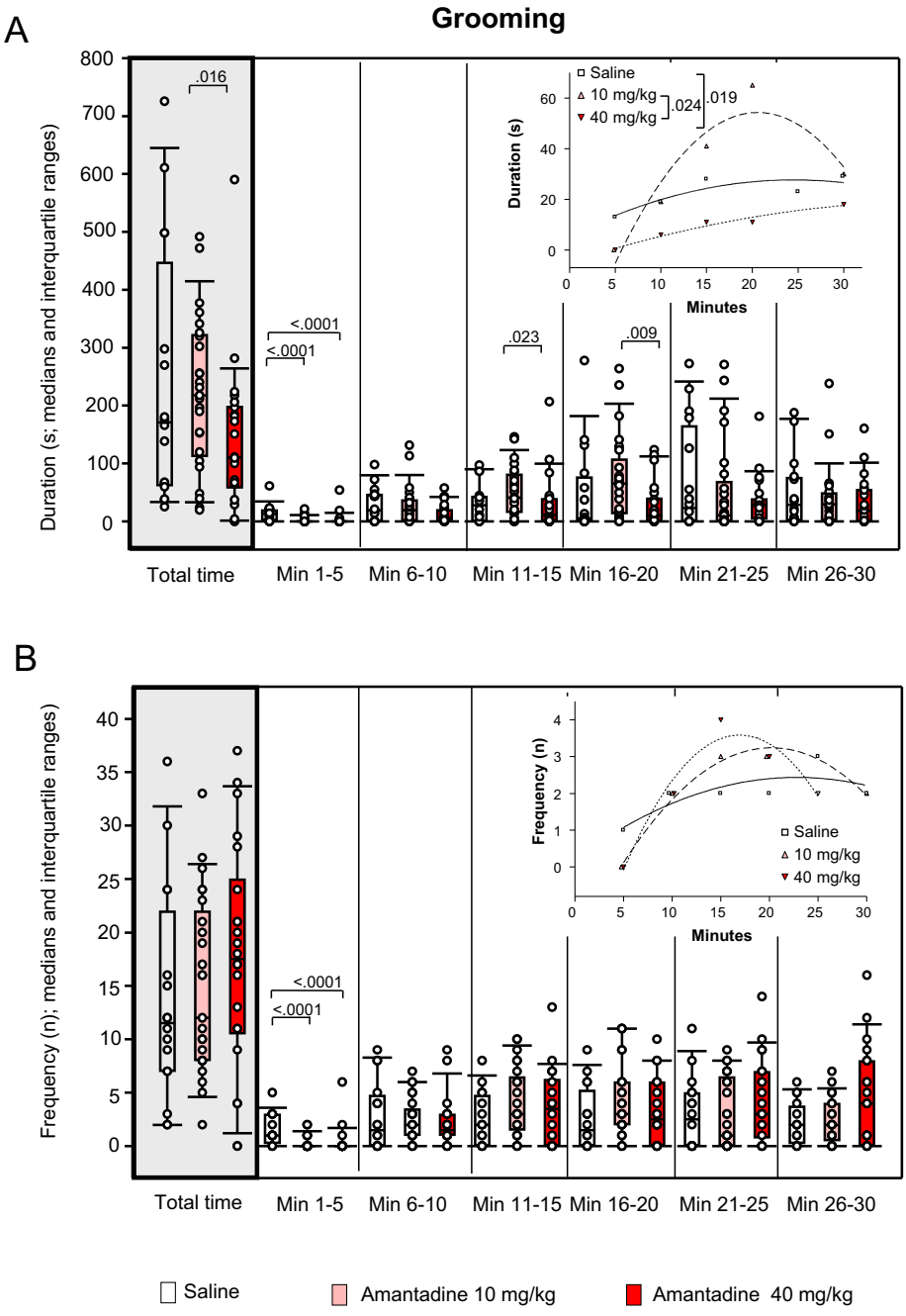

Fig. 8. Grooming. Duration (s) and Frequency (n) after vehicle (0.9% saline, white), 10 mg/kg amantadine (pink) and 40 mg/kg amantadine (red). The figure shows box and whisker plots of the median durations (A) and frequencies (B) of grooming during the whole time of testing (grey shade) and in the individual 5-min time bins. 25-/75-percentiles are given in the boxes, while 5-/95-percentiles are represented by the whiskers. The circles represent the individual animals. Between-group differences were assessed using the Mann-Whitney *U* test (two-tailed). p values ≤ 0.05 are given in the figure. Due to the Bonferroni correction, p values ≤ 0.0167 are considered significant. *Inset*: Time-behavior curves (saline, white squares; 10 mg/kg amantadine, pink triangles; 40 mg/kg amantadine, red triangles) were obtained by plotting median values of grooming durations (A) and frequencies (B) against time by plotting median values of sitting durations (A) and sitting frequencies (B) against time and fitting quadratic functions [$y(t) = a + bt + ct^2$ with a, absolute term; b, linear term; c, quadratic term] to these data. Between-group differences were assessed using the *F* test (two-tailed). p values ≤ 0.05 are given in the inset. Due to the Bonferroni correction, p values ≤ 0.0167 are considered significant. (For interpretation of the references to color in this figure legend, the reader is referred to the web version of this article.)

reduction of DA efflux, a subsequent reduction of feedback inhibition and the compensatory enhancement of DA release. Also for the NAC it may be assumed that GLUergic and GABAergic mechanisms occur simultaneously, incurring a net increase of synaptic DA, as reflected by the decreased of neostriatal $D_{2/3}R$ binding in the NAC relative to baseline.

The elevation of GABA levels in the SN (Bak et al., 1972) can be assumed to block DA release in this region. Moreover, the increased availability of GABA in the CP likely increases both inhibition and disinhibition of the SN via the direct and indirect pathway, respectively. Both inhibitory and disinhibitory actions on the SN are also exerted by the STN, which sends GLUergic efferents to SNr and GP, and receives GLUergic input from the neocortex (Hammond et al., 1978; Canteras et al., 1990). A further inhibition is caused by the GABAergic thalamonigral fibers, while excitatory as well as inhibitory actions can be ascribed to the DAergic striatonigral and striatopallidal efferents dependent on their course (direct vs indirect pathway; for review see, Hauber, 1998). Additionally, the GP receives GABAergic input from the NAC (Yamamoto et al., 1983), incurring a disinhibition of the VTA. Apparently, in sum, these effects balanced each other, leaving $D_{2/3}R$ binding in the SN/VTA unaltered relative to baseline after treatment with either dose of AMA.

DA fibers in the direct and indirect pathway are considered to exert tonic inhibition of the THAL (Crossman, 1987; Albin et al., 1989; DeLong, 1990). Consequently, the increased DAergic input from the CP - together with the increased GABAergic input from both CP and NAC - could result in a net inhibition of the THAL, ensueing in a reduction of DA efflux, a subsequent decline of feedback inhibition and a compensatory enhancement of DA release, resulting in the observed decrease $D_{2/3}R$ binding in the THAL after 40 mg/kg AMA.

Probably, the lower dose of AMA released less GLU, DA and GABA in the NAC compared to the higher dose. This, in sum, left accumbal $D_{2/}$

$_3$R binding after 10 mg/kg AMA unaltered relative to baseline. The NAC receives DA afferents from limbic regions including the HIPP and sends DAergic projections back to them (Graybiel and Ragsdale Jr., 1979; Nazari-Serenjeh et al., 2011). Consequently, reduced GLU and DA levels in the NAC can be hypothesized to result in a decrease of DAergic input to the HIPP, which may have led to a compensatory elevation of DA efflux relative to the higher AMA dose as reflected by the reduced $D_{2/3}$R binding in this region. In turn, increased DAergic input from the HIPP may have compensatorily reduced DA release in the NAC, thus contributing to the unaltered amount of $D_{2/3}$R binding relative to baseline. The reduction of available GABA decreased the inhibition of the GP and the subsequent disinhibition of the THAL relative to the higher AMA dose. Probably, this resulted in a lessening of NAC inhibition and an increase of DA release, which was sufficient to induce the observed behavioral alterations (reduction of ambulation and rearing duration and increase of sitting duration and frequency in the first 5 min post-challenge), but not high and/or long enough to reduce [^{123}I]IBZM binding at the time of SPECT acquisition.

4.4. Appraisal

AMA affects both DA levels and animal behavior immediately post-injection (Maj et al., 1972; Takahashi et al., 1996), while the method of in vivo SPECT inherently requires a sufficient time for the radioligand to accumulate. Combining the assessment of behavior with $D_{2/3}$R imaging, thus, allows to study the effects of DA as elicited by the NMDAR antagonist in a continuous fashion, with the outcome of behavioral and in vivo imaging studies mutually predicting each other.

In the present study, the NMDAR antagonist AMA reduced $D_{2/3}$R binding (and increased DA) in relevant regions of the nigrostriatal and mesolimbic system. The decrement of ambulatory and exploratory activity after 40 mg/kg AMA, which was more intense, more rapid and extended over a longer time compared to both saline and the lower dose, suggests that the higher dose of AMA elicited a general behavioral depression. Under normal conditions, DA disinhibits the GABAergic neurons of the direct pathway (CP – pars reticulata of the SN/internal GP), leading to an activation of the mesencephalic, diencephalic and brainstem motor centers, whereas, in the indirect pathway (CP – external GP/subthalamic nucleus - pars reticulata of the SN/internal GP), DA inhibits GABAergic neurons resulting in a suppression of motor activity (for review see Grillner and Robertson, 2015). From this may be inferred that, after the higher AMA dose, the increased availability of DA (probably caused by the increased GLUergic and GABAergic input to CP and NAC) in the nigrostriatal and mesolimbic pathway ultimately effectuated an inhibition of motor neurons. Furthermore, the NAC with its limbic DAergic afferents and its efferents to the GP is believed to act as a limbic-motor interface relevant for the translation of emotional/motivational states into action (for review see Mogenson et al., 1980). Since the increased availability of DA in the NAC may have incurred a decrease of DAergic activity in the target regions of mesolimbic DAergic projections, also an inhibitory influence of AMA on the motivational drive may not be excluded.

The decrease of exploratory activities such as rearing and head-shoulder motility as well as the increase of sitting behavior within or between trials is generally considered to reflect behavioral habituation (for review see Leussis and Bolivar, 2006). In the present study, motor/exploratory activity increased after 40 mg/kg AMA towards the end of the testing time. This is illustrated by the higher final values of the t-b curves of ambulation duration, ambulation frequency as well as duration and frequency of head-shoulder motility compared to the other treatments. Besides, the curve of duration of head-shoulder motility exhibited a dramatic rise, while the curves obtained after 10 mg/kg AMA and saline declined over time. This implies, that the NMDAR antagonist AMA, at least in the higher dose, prevented behavioral habituation. Further studies using explicit learning tasks are required in order to assess the mnemogenic effects of AMA and their dose-dependency.

In the present investigation, we employed a MRI-based mode of analysis, which not only allows the definition of exact anatomical VOIs within the striatum (CP, NAC), but also the definition of VOIs other than striatal ones, which are either smaller or display lower densities of D_2R-like binding sites such as SN/VTA, THAL or HIPP. The maximum VOI diameters are either in the range of or beyond the spatial resolution of the "TierSPECT". It must be considered, however, that in those portions of VOIs, whose diameters are smaller than the full width at half maximum, the exact quantification of $D_{2/3}$R binding may be hampered by partial volume effects leading to underestimations of radioligand accumulation. A further source of error may be spill-over from regions with high radioligand accumulation such as the extraorbital Harderian glands to the adjacent VOIs of FC, CP and NAC, or from the CP to NAC, THAL and aHIPP, causing overestimations of radioligand binding. However, since this pertains to SPECT measurements both in baseline and after challenge, the exactitude of (semi)quantitative values in either condition, but not the comparability of data between baseline and challenge may have been biassed.

Another pitfall of the present investigation may have been the employment of ketamine as anaesthetic. This compound also acts as an NMDA antagonist and has been shown to enhance DA efflux in rats (e.g., Müller et al., 2011) as well as to reduce $D_{2/3}$ receptor binding in healthy subjects (Breier et al., 1998). Hence, it cannot be excluded that DA release induced by ketamine contributed to the reduction of $D_{2/3}$ receptor binding observed in the present investigation. Since the same anaesthetic was used in baseline and after challenge, data basically remain comparable. However, further studies are required in order to assess possible additive or opposed actions of amantadine and ketamine in various dosages.

The present study determined regional changes of synaptic DA after AMA by assessing alterations of $D_{2/3}$R binding relative to baseline. Our hypotheses of GLU, DA and GABA interactions are preliminary, and further studies are needed to clarify, how exactly the observed changes were effected. This not only pertains to likely contributions of other neurotransmitter systems (such as the AChergic [Bak et al., 1972], 5-HTergic [Bak et al., 1972] and/or opioid system [Peeters et al., 2004]), but also to the exact mode of action of AMA, which may involve processes as diverse as stimulation of DOPA decarboxylase activity (Deep et al., 1999) and the increase of presynaptic DA transporter binding sites (Tsukada et al., 2001).

5. Conclusions

In sum, results show reductions of $D_{2/3}$R binding in regions of the nigrostriatal and mesolimbic system (NAC, CP, THAL, aHIPP) of the rat after challenge with the NMDAR antagonist AMA, which may be conceived to reflect an increased availability of DA. Thereby, decreases of $D_{2/3}$R binding (and increases of DA) are associated with a reduction of motor/exploratory activity in the first 15 min post-challenge. Findings may be relevant for the treatment of neurological and psychiatric conditions such as Parkinson's disease, Huntington's disease or schizophrenia, which are characterized by both DAergic and GLUergic dysfunction.

Author contributions

Experimental design: SN, MAdSS, JPH, GA and HWM. Performance of imaging and behavioral studies: SN, HJW, AML and FW. Evaluation and statistical analysis: SN and MB.

Interpretation of findings: SN, MB, CA, MAdSS, JPH, HWM. Writing and editing of the manuscript: SN, HJW, CA, MAdSS, JPH, HH, HWM.

Conflict of interest statement

The authors declare that they have no conflict of interest.

Acknowledgements

MAdSS was supported by a Heisenberg Fellowship SO 1032/5-1 and EU-FP7 (MC-ITN-"In-SENS"-ESR7 607616). JPH was supported by "Deutsche Forschungsgemeinschaft" (Grant: DFG HU 306/27-3).

References

Albin, R.L., Young, A.B., Penney, J.B., 1989. The functional anatomy of basal ganglia disorders. Trends Neurosci. 12, 366–375.
Archer, T., Garcia, D., 2016. Attention-deficit/hyperactivity disorder: focus upon aberrant N-methyl-D-aspartate receptors systems. Curr. Top. Behav. Neurosci. 29, 295–311.
Bak, I.J., Hassler, R., Kim, J.S., Kataoka, K., 1972. Amantadine actions on acetylcholine and GABA in striatum and substantia nigra of rat in relation to behavioral changes. J. Neural Transm. 33, 45–61.
Breier, A., Adler, C.M., Weisenfeld, N., Su, T.P., Elman, I., Picken, L., Malhotra, A.K., Pickar, D., 1998. Effects of NMDA antagonism on striatal dopamine release in healthy subjects: application of a novel PET approach. Synapse 29, 142–147.
Buus Lassen, J., 1973. The effect of amantadine and (+)-amphetamine on motility in rats after inhibition of monoamine synthesis and storage. Psychopharmacologia (Berl.) 29, 55–64.
Canteras, N.S., Shammah-Lagnado, S.J., Silva, B.A., Ricardo, J.A., 1990. Afferent connections of the subthalamic nucleus: a combined retrograde and anterograde horseradish peroxidase study in the rat. Brain Res. 513, 43–59.
Crossman, A.R., 1987. Primate models of dyskinesia: the experimental approach to the study of basal ganglia-related involuntary movement disorders. Neuroscience 21, 1–40.
de Souza Silva, M.A., Topic, B., Huston, J.P., Mattern, C., 2008. Intranasal administration of progesterone increases dopaminergic activity in amygdala and eostriatum of male rats. Neuroscience 157, 196–203.
de Souza Silva, M.A., Mattern, C., Topic, B., Buddenberg, T.E., Huston, J.P., 2009. Dopaminergic and serotonergic activity in neostriatum and nucleus accumbens enhanced by intranasal administration of testosterone. Eur. Neuropsychopharmacol. 19, 53–63.
Deep, P., Dagher, A., Sadikot, A., Gjedde, A., Cumming, P., 1999. Stimulation of dopa decarboxylase activity in striatum of healthy human brain secondary to NMDA receptor antagonism with a low dose of amantadine. Synapse 34, 313–318.
DeLong, M.R., 1990. Primate models of movement disorders of basal ganglia origin. Trends Neurosci. 13, 281–285.
Fink, J.S., Smith, G.P., 1979. L-Dopa repairs deficits in locomotor and investigatory exploration produced by denervation of catecholamine terminal fields in the forebrain of rats. J. Comp. Physiol. Psychol. 93, 66–73.
Gibbs, T., Russek, S., Farb, D., 2006. Sulfated steroids as endogenous neuromodulators. Pharmacol. Biochem. Behav. 84, 555–567.
Graybiel, A.M., Ragsdale Jr., C.W., 1979. Fiber connections of the basal ganglia. Prog. Brain Res. 51, 237–283.
Grigoriadis, N., Simeonidou, C., Parashos, S.A., Albani, M., Guiba-Tziampiri, O., 1996. Ontogenetic development of the locomotor response to levodopa in the rat. Pediatr. Neurol. 14, 41–55.
Grillner, S., Robertson, B., 2015. The basal ganglia downstream control of brainstem motor centres—an evolutionarily conserved strategy. Curr. Opin. Neurobiol. 33, 47–52.
Groves, P.M., 1983. A theory of the functional organization of the neostriatum and the neostriatal control of voluntary movement. Brain Res. 5, 109–132.
Haase, A., Frahm, J., Matthaei, D., Hänicke, W., Merboldt, K.D., 1986. FLASH imaging. Rapid NMR imaging using low flip-angle pulses. J. Magn. Reson. 67, 258–266.
Hammond, C., Deniau, J.M., Rizk, A., Feger, J., 1978. Electrophysiological demonstration of an excitatory subthalamonigral pathway in the rat. Brain Res. 151, 235–244.
Hara, M., Sasa, M., Takaori, S., 1989. Ventral tegmental area-mediated inhibition of neurons of the nucleus accumbens receiving input from the parafascicular nucleus of the thalamus is mediated by dopamine D1 receptors. Neuropharmacology 28, 1203–1209.
Hauber, W., 1998. Involvement of basal ganglia transmitter systems in movement initiation. Prog. Neurobiol. 56, 507–540.
Ichise, M., Meyer, J.H., Yonekura, Y., 2001. An introduction to PET and SPECT neuroreceptor quantification models. J. Nucl. Med. 42, 755–763.
Johnson, T.N., Rosvold, H.E., Mishkin, M., 1968. Projections from behaviorally-defined sectors of the prefrontal cortex to the basal ganglia, septum, and diencephalon of the monkey. Exp. Neurol. 21, 20–34.
Konradi, C., Heckers, S., 2003. Molecular aspects of glutamate dysregulation: implications for schizophrenia and its treatment. Pharmacol. Ther. 97, 153–179.
Kornhuber, J., Weller, M., 1997. Psychotogenicity and N-methyl-D-aspartate receptor antagonism: implications for neuroprotective pharmacotherapy. Biol. Psychiatry 41, 135–144.
Kornhuber, J., Bormann, J., Hübers, M., Rusche, K., Riederer, P., 1991. Effects of the 1-amino-adamantanes at the MK-801-binding site of the NMDA-receptor-gated ion channel: a human postmortem brain study. Eur. J. Pharmacol. 206, 297–300.
Kornhuber, J., Schoppmeyer, K., Riederer, P., 1993. Affinity of 1-aminoadamantanes for the sigma binding site in post-mortem human frontal cortex. Neurosci. Lett. 163, 129–131.
Kornhuber, J., Quack, G., Danysz, W., Jellinger, K., Danielczyk, W., Gsell, W., Riederer, P., 1995. Therapeutic brain concentration of the NMDA receptor antagonist amantadine. Neuropharmacology 34, 713–721.
Langer, S.Z., 1974. Presynaptic regulation of catecholamine release. Biochem. Pharmacol. 23, 1793–1800.
Laruelle, M., 2000. Imaging synaptic neurotransmission with in vivo binding competition techniques: a critical review. J. Cereb. Blood Flow Metab. 20, 423–451.
Leussis, M.P., Bolivar, V.J., 2006. Habituation in rodents: a review of behavior, neurobiology, and genetics. Neurosci. Biobehav. Rev. 30, 1045–1064.
Maj, J., Sowińska, H., Baran, L., 1972. The effect of amantadine on motor activity and catalepsy in rats. Psychopharmacologia 24, 296–307.
McDevitt, J.T., Setler, P.E., 1981. Differential effects of dopamine agonists in mature and immature rats. Eur. J. Pharmacol. 72, 69–75.
Mitchell, N.D., Baker, G.B., 2010. An update on the role of glutamate in the pathophysiology of depression. Acta Psychiatr. Scand. 122, 192–210.
Mogenson, G.J., Jones, D.L., Yim, C.Y., 1980. From motivation to action: functional interface between the limbic system and the motor system. Prog. Neurobiol. 14, 69–97.
Moresco, R.M., Volonte, M.A., Messa, C., Gobbo, C., Galli, L., Carpinelli, A., Rizzo, G., Panzacchi, A., Franceschi, M., Fazio, F., 2002. New perspectives on neurochemical effects of amantadine in the brain of parkinsonian patients: a PET - [(11)C]raclopride study. J. Neural Transm. (Vienna) 109, 1265–1274.
Moryl, E., Danysz, W., Quack, G., 1993. Potential antidepressive properties of amantadine, memantine and bifemelane. Pharmacol. Toxicol. 72, 394–397.
Müller, C.P., Thönnessen, H., Jochamm, G., Barrosm, M., Tomaz, C., Carey, R.J., Huston, J.P., 2004. Cocaine-induced 'active immobility' and its modulation by the serotonin1A receptor. Behav. Pharmacol. 15, 481–493.
Müller, C.P., Pum, M.E., Amato, D., Schüttler, J., Huston, J.P., Silva, M.A., 2011. The in vivo neurochemistry of the brain during general anesthesia. J. Neurochem. 119, 419–446.
Navarrete, R., Slawińska, U., Vrbová, G., 2002. Electromyographic activity patterns of ankle flexor and extensor muscles during spontaneous and L-DOPA-induced locomotion in freely moving neonatal rats. Exp. Neurol. 173, 256–265.
Nazari-Serenjeh, F., Rezayof, A., Zarrindast, M.R., 2011. Functional correlation between GABAergic and dopaminergic systems of dorsal hippocampus and ventral tegmental area in passive avoidance learning in rats. Neuroscience 24, 104–114.
Nikolaus, S., Larisch, R., Wirrwar, A., Yamdjeu-Nouné, M., Antke, C., Beu, M., Schramm, N., Müller, H.W., 2005. [^{123}I]Iodobenzamide binding to the rat dopamine D_2 receptor in competition with haloperidol and endogenous dopamine – an in vivo imaging study with a dedicated small animal SPECT. Eur. J. Nucl. Med. Mol. Imaging 32, 1305–1310.
Nikolaus, S., Beu, M., Hautzel, H., De Souza Silva, M.A., Wirrwar, A., Antke, C., Huston, J.P., Müller, H.W., 2013. Effects of L-DOPA on striatal iodine-123-FP-CIT binding and behavioral parameters in the rat. Nucl. Med. Commun. 34, 1223–1232.
Nikolaus, S., Beu, M., De Souza Silva, A.M., Huston, J.P., Hautzel, H., Mattern, C., Antke, C., Müller, H.W., 2016. Relationship between L-DOPA-induced reduction in motor and exploratory activity and striatal dopamine D_2 receptor binding in the rat. Front. Behav. Neurosci. 9, 352.
Nikolaus, S., Beu, M., de Souza Silva, M.A., Huston, J.P., Antke, C., Müller, H.W., Hautzel, H., 2017. GABAergic control of neostriatal dopamine D_2 receptor binding and behaviors in the rat. Pharmacol. Biochem. Behav. 153, 76–87.
Nikolaus, S., Wittsack, J., Beu, M., De Souza Silva, M.A., Huston, J.P., Müller-Lutz, A., Wickrath, F., Antke, C., Antoch, G., Müller, H.W., Hautzel, H., 2018a. GABAergic control of nigrostriatal and mesolimbic dopamine in the rat brain. Front. Behav. Neurosci. 12, 38.
Nikolaus, S., Beu, M., Antke, C., Müller, H.W., 2018b. Translating neurochemistry: benefit of joint behavioral and in vivo imaging studies in the rat for neuropsychiatric disorders. J. Translat. Sci. 5, 1–3.
Paxinos, G., Watson, C., 2014. The Rat Btain in Stereotaxix Coordinates, 7th edition. Academic Press, Elesevier, Amsterdam.
Peeters, M., Romieu, P., Maurice, T., Su, T.P., Maloteaux, J.M., Hermans, E., 2004. Involvement of the sigma 1 receptor in the modulation of dopaminergic transmission by amantadine. Eur. J. Neurosci. 19, 2212–2220.
Powell, E.W., Leman, R.B., 1976. Connections of the nucleus accumbens. Brain Res. 105, 389–403.
Quack, G., Hesselink, M., Danysz, W., Spanagel, R., 1995. Microdialysis studies with amantadine and memantine on pharmacokinetics and effects on dopamine turnover. J. Neural Transm. Suppl. 46, 97–105.
Rebec, G.V., 2018. Corticostriatal network dysfunction in Huntington's disease: deficits in neural processing, glutamate transport, and ascorbate release. CNS Neurosci. Ther. 24, 281–291.
Scatton, B., Cheramy, A., Besson, M.J., Glowinski, J., 1970. Increased synthesis and release of dopamine in the striatum of the rat after amantadine treatment. Eur. J. Pharmacol. 13, 131–133.
Schiffer, W.K., Mirrione, M.M., Biegon, A., Alexoff, D.L., Patel, V., Dewey, S.L., 2006. Serial microPET measures of the metabolic reaction to a microdialysis probe implant. J. Neurosci. Methods 155, 272–284.
Schramm, N., Wirrwar, A., Sonnenberg, F., Halling, H., 2000. Compact high resolution detector for small animal SPECT. IEEE Trans. Nucl. Sci. 47, 1163–1166.
Seneca, N., Finnema, S.J., Farde, L., Gulyás, B., Wikström, H.V., Halldin, C., Innis, R.B., 2006. Effect of amphetamine on dopamine D2 receptor binding in nonhuman primate brain: a comparison of the agonist radioligand [11C]MNPA and antagonist [11C] raclopride. Synapse 59, 260–269.
Shaygannejad, V., Janghorbani, M., Ashtari, F., Zakeri, H., 2012. Comparison of the effect of aspirin and amantadine for the treatment of fatigue in multiple sclerosis: a randomized, blinded, crossover study. Neurol. Res. 34, 854–858.
Spritzer, S.D., Kinney, C.L., Condie, J., Wellik, K.E., Hoffman-Snyder, C.R., Wingerchuk, D.M., Demaerschalk, B.M., 2015. Amantadine for patients with severe traumatic brain injury: a critically appraised topic. Neurologist 19, 61–64.
Takahashi, T., Yamashita, H., Zhang, Y.X., Nakamura, S., 1996. Inhibitory effect of MK-

801 on amantadine-induced dopamine release in the rat striatum. Brain Res. Bull. 41, 363–367.
Tsukada, H., Nishiyama, S., Kakiuchi, T., Ohba, H., Sato, K., Harada, N., 2001. Ketamine alters the availability of striatal dopamine transporter as measured by [(11)C]beta-CFT and [(11)C]beta-CIT-FE in the monkey brain. Synapse 42, 273–280.
Ueki, A., Uno, M., Anderson, M., Yoshida, M., 1977. Monosynaptic inhibition of thalamic neurons produced by stimulation of the substantia nigra. Experientia 33, 1480–1488.
Vanle, B., Olcott, W., Jimenez, J., Bashmi, L., Danovitch, I., IsHak, W.W., 2018. NMDA antagonists for treating the non-motor symptoms in Parkinson's disease. Transl. Psychiatry 2018 (8), 117.
Verhoeff, N.P.L.G., Bobeldijk, M., Feenstra, M.P.G., Boer, G.J., Maas, M.A.W., Erdtsieck-Ernste, E., De Bruin, K., Van Royen, E.A., 1991. In vitro and in vivo D_2-dopamine receptor binding with (^{123}I)IBZM) in rat and human brain. Int. J. Rad. Appl. Instrum. B 18, 837–846.
Videbaek, C., Toska, K., Scheideler, M.A., Paulson, O.B., Moos Knudsen, G., 2000. SPECT tracer [(^{123})I]IBZM has similar affinity to dopamine D2 and D3 receptors. Synapse 38, 338–342.
Vishnoi, S., Raisuddin, S., Parvez, S., 2016. Glutamate excitotoxicity and oxidative stress in epilepsy: modulatory role of melatonin. J. Environ. Pathol. Toxicol. Oncol. 35, 365–374.
Volonté, M.A., Moresco, R.M., Gobbo, C., Messa, C., Carpinelli, A., Rizzo, G., Comi, G., Fazio, F., 2001. A PET study with [11-C]raclopride in Parkinson's disease: preliminary results on the effect of amantadine on the dopaminergic system. Neurol. Sci. 22, 107–108.
Wilson, R.B., Eliyan, Y., Sankar, R., Hussain, S.A., 2018. Amantadine: a new treatment for refractory electrical status epilepticus in sleep. Epilepsy Behav. 84, 74–78.
Yamamoto, T., Hassler, R., Huber, C., Wagner, A., Sasaki, K., 1983. Electrophysiologic studies on the pallido- and cerebellothalamic projections in squirrel monkeys (*Saimiri sciureus*). Exp. Brain Res. 51, 77–87.